FOCUSED ULTRASOUND TREATMENT OF GLIOBLASTOMA

by
Molly Acord

A thesis submitted to Johns Hopkins University in conformity
with the requirements for the degree of Master of Science in Engineering

Baltimore, Maryland
MAY 2021

Abstract

Glioblastoma (GB) remains one of the most difficult challenges for neurosurgeons due to its highly vascularized and complex characteristics. Focused ultrasound (FUS) is quickly being integrated into GB research thanks to its ability to treat tumors a distance away from the transducer without harming healthy tissues in its path.

Presented here is a comprehensive review of FUS therapies for GB treatment. Therapies include thermal ablation, blood-brain barrier opening, radiosensitization, sonodynamic therapy, and immunomodulation, all of which have the potential to change GB treatment regimens.

This thesis reports a minimally invasive high-intensity focused ultrasound (HIFU) probe designed for brain surgery. It has been reduced in size from its previous generation and now possesses steering capabilities in the axial direction. This could take the place of some recurrent GB resection surgeries.

Also presented here is a phantom study for a commercial magnetic resonance guided focused ultrasound system, the RK-300, which has the ability to perform most of the therapies mentioned above. The phantom study confirms the functionality of the system, which after lying dormant for a few years is now ready for laboratory research.

In transitioning FUS to the clinical setting, there needs to be real-time methods of monitoring surrounding tissue. Here, a fiber optic temperature sensor the width of a human hair is tested and validated for monitoring temperature conditions in the

central nervous system.

Thesis Readers

Dr. Amir Manbachi (Co-Primary Advisor)
Assistant Professor
Department of Biomedical Engineering
Department of Electrical Engineering
Department of Neurosurgery
Johns Hopkins University
Johns Hopkins School of Medicine

Prof. Betty Tyler
Associate Professor (Co-Primary Advisor)
Department of Neurosurgery
Johns Hopkins University
Johns Hopkins School of Medicine

Dr. Raj Mukherjee
Assistant Professor
Department of Neurosurgery
Johns Hopkins School of Medicine
Director of Neurosurgical Oncology
Johns Hopkins Bayview Medical Center

"It is not the critic who counts; not the man who points out how the strong man stumbles, or where the doer of deeds could have done them better. The credit belongs to the man who is actually in the arena, whose face is marred by dust and sweat and blood; who strives valiantly; who errs, who comes short again and again, because there is no effort without error and shortcoming; but who does actually strive to do the deeds; who knows great enthusiasms, the great devotions; who spends himself in a worthy cause; who at the best knows in the end the triumph of high achievement, and who at the worst, if he fails, at least fails while daring greatly, so that his place shall never be with those cold and timid souls who neither know victory nor defeat."

-Theodore Roosevelt

Acknowledgements

Thank you to my advisors, Amir Manbachi and Betty Tyler. I would not have been able to do this without your continued encouragement and support. Dr. Manbachi, you took a chance on me in the very beginning and I can't tell you enough how much I appreciate the world that you have introduced me to. Betty, I am so happy to have worked with you during this phase of my life. You've taught us how to handle crazy rats, stayed with us when we've been worried cell parents, and gave us the freedom to try new things. I hope to be half of the researcher and mentor you are one day.

Thank you to Desmond Jacob for all of your long hours with us at the MRI and for being patient and helpful. Thank you to Marc Santos and Rajiv Chopra for your long zoom calls and emails exchanged to help get the RK-300 working properly. Thank you to Austin Devinney and George Coles at The Johns Hopkins Applied Physical Laboratory for your continued support of the fiber optic temperature sensor and your wonderful mentorship. Thank you to The Johns Hopkins University, the biomedical engineering department, and the neurosurgery department. I would like to acknowledge funding support from the Department of Neurosurgery, National Science Foundation (NSF) STTR Phase 1 Award (#: 1938939), Defense Advanced Research Projects Agency (DARPA) Award (#: N660012024075), and Johns Hopkins Institute for Clinical and Translational Research (ICTR)'s Clinical Research Scholars Program (KL2), administered by the National Institutes of Health (NIH) National Center for Advancing Translational Sciences (NCATS).

Thank you to my momma who is always encouraging and loves me unconditionally.

Thank you to my dearest friends, Alisa and Nina, who help me remember to have fun and not take life too seriously. To my fur babies: My dearest Fran, I miss you every day and my sweet Cookie, you have given me so much joy already.

Finally, I want to thank my right-hand person, my balance, who I could never have done any of this without: Tarana Kaovasia. You've been with me every day throughout this journey, enduring many ups and downs, yet you continue to have the same enthusiasm as you did on day one. You were meant for this world of research. I have no doubt that you will one day mentor students like us and help them achieve their dreams. Good luck my beta.

Contents

List of Tables

List of Figures

Chapter 1

Introduction

Glioblastoma

Overview

Neoplasms, commonly known as tumors, are an abnormal growth of tissue that arises from continuous cell division or prolonged cell survival. Benign neoplasms may grow to a considerable size, which may lead to other serious issues, but do not invade surrounding tissues or typically metastasize. Malignant neoplasms, in addition to growing, invade surrounding tissues and frequently have a propensity to metastasize to other organs [1]. Neuro-oncology is the study and treatment of neoplasms that involve the brain or spinal cord, including, but are not limited to meningiomas, oligodendrogliomas, astrocytomas, medulloblastomas, and glioblastomas [2]. GBs are the most common malignant primary brain tumors, accounting for 50% of primary malignant brain tumors and 15% of all central nervous system tumors [3]. GBs are aggressive, invasive, and result in the shortest patient survival rate for malignant brain tumors (as seen in Table 1-I).

Table 1-I. Brain Tumor Average 5 Year Survival

Tumor Type	Average 5 Year Survival Rate (%) [4]
Low Grade (Diffuse) Astrocytoma	45
Anaplastic Astrocytoma	33
Oligodendroglioma	79
Anaplastic Oligodendroglioma	59
Ependymoma/Anaplastic Ependymoma	89
Meningioma	78
GB	11

Clinical Treatment Regimen Today

Conventional therapies are aimed at removing, reducing, or slowing the growth of the tumor mass. Radiation therapy uses high doses of radiation to kill cancer cells and to slow the growth of cancer by destroying its DNA. External radiotherapy is the most common form of radiation treatment and the least invasive, as it aims an external beam of radiation at a specific cancer region. The other form of radiation therapy is internal radiation, which is more invasive and involves potential risks. In this treatment, radiation is injected into the body via a solid or liquid and works to destroy the cancer; but unfortunately, this may also harm healthy cells [5]. Oftentimes radiation is used in combination with surgical resection and/or chemotherapy to treat GBs. Radiation alone or with initial surgery typically only results in a survival of 12 months [6]. Radiation combined with chemotherapy usually only increases that survival time to 15 months [6].

Chemotherapy is a cancer treatment that uses chemotherapeutic agents to kill cells that grow and divide quickly, typically a selective characteristic of cancer cells. These particular drugs can be administered in various ways: infusions, injections, pills, creams, specific cavity injections, and dissolvable wafers [7]. Chemotherapy is often successful in treating various types of cancer, but faces a major challenge when it comes to brain cancer: the blood-brain barrier (BBB). The BBB is a protective

element between circulating blood and neural tissue, keeping possible toxins and pathogens separated from the brain. It consists of endothelial cells which form tight junctions, only allowing small agents through to the brain [8]. Chemotherapy agents are often too large to cross the BBB and thus, are not an appropriate noninvasive form of treatment. Among the few agents that can cross the BBB, temozolomide (TMZ) is a common choice for treatment. However, in patients with early GB diagnosis, TMZ is only shown to increase survival time by 2.5 months [4]. To account for the BBB challenge, oftentimes after surgical resection of the tumor, wafers are placed in the surrounding area to gradually release chemotherapy agents in the cancer area over time [9].

Surgical procedures that are performed include biopsies and resections. Biopsies, typically needle biopsies for GBs, can determine pathological diagnosis of the tumor mass and help guide treatment [10]. Resections are generally performed in an attempt to remove the tumor mass. However, due to the infiltrative nature of GBs, even apparent gross total resections are unable to excise all of the tumor cells, often resulting in tumor recurrence [11]. Therefore, for the treatment of GBs, resections are aimed to relieve the mass effect of the tumor [10, 11]. Craniotomies, both asleep and awake, are the most common surgical procedures in the treatment of GBs [10]. Maximally resected tumors result in an improved prognosis. Greater than 70% of tumor volumes excised are accompanied by a statistically significant survival rate [12], with a larger than 90% extent of resection having a greater one-year survival rate. Excised tumor volumes larger than 95% may be difficult to achieve and may risk neurological deficits [11]. Maximal tumor resection is often followed by radiation and/or chemotherapy [10]. Resections are considerably invasive and risky. Complications like neurological deficits can affect quality of life and unclear resection margins can cause the tumor to recur [12]. Resection as a treatment option is sometimes excluded if the tumor is deep seated or surrounded by eloquent brain matter [11].

The above-mentioned drawbacks arising from conventional therapies drives the need for more minimally invasive methods with reduced physiological side-effects. FUS has has been shown to be a competent tool in alternative therapy and has hence been gaining traction.

Focused Ultrasound

Basic Principles

Ultrasound refers to sound waves at frequencies greater than the human auditory range (>20,000 Hz). Ultrasound transducers, comprised of piezoelectric crystals, vibrate when exposed to voltage. The waves generated from the vibrations travel throughout the medium in contact with the transducer and cause the medium to vibrate at the same frequency. In sonography applications, transducers are flat or convex and can receive the response waves generated from the vibrating medium to reconstruct an image. In FUS, the transducers are concave, so the ultrasound waves emitted converge at a focal point within the medium. The acoustic energy at this focal point can be used for various therapies (see Fig. 1-1) specific to treatments for GB: thermal ablation, chemotherapy-aided BBB opening, radiosensitization, sonodynamic therapy (SDT), immunomodulation, etc.

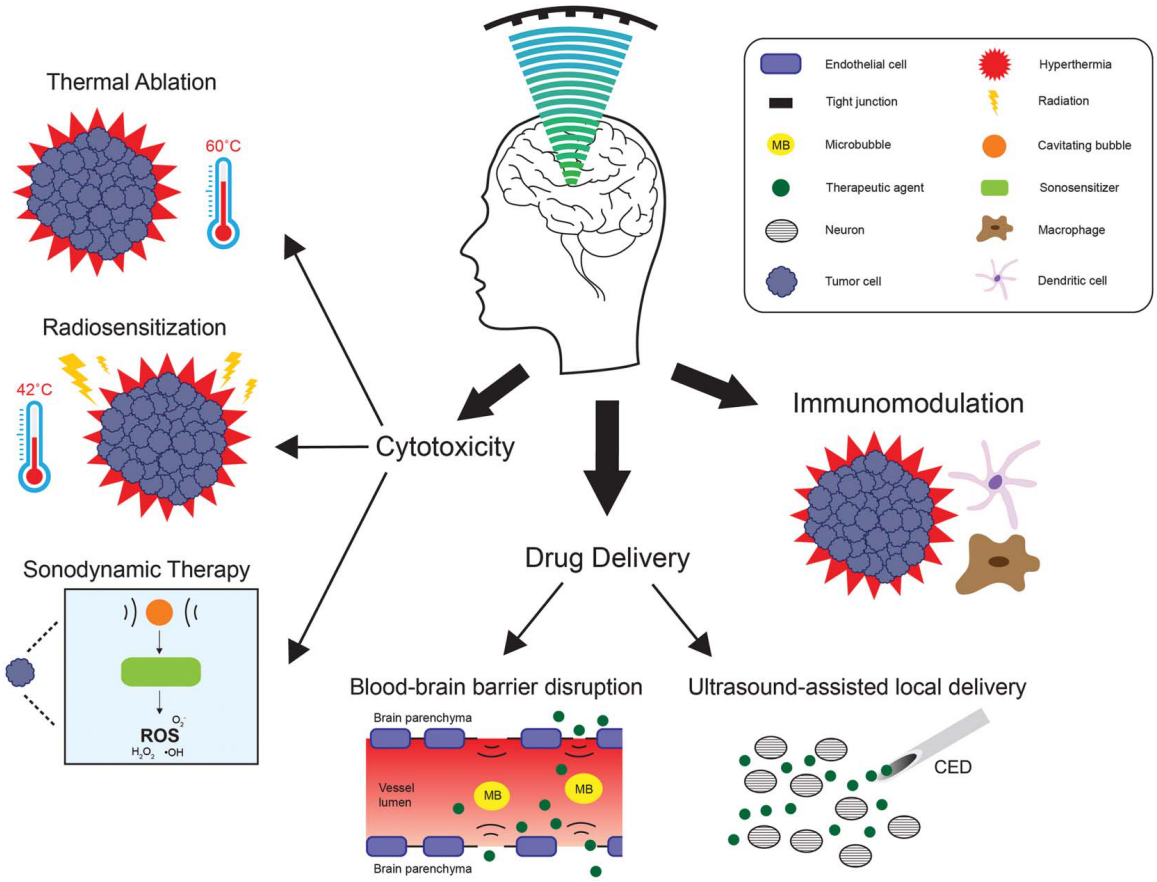

Figure 1-1. Treatment for GB: Applications of Focused Ultrasound (reproduced with permission from [13])

Thermal Ablation

Thermal ablation requires the use of HIFU to generate temperatures capable of resulting in tissue death, also known as necrosis. Temperatures above 60°C can easily cause instantaneous necrosis for most cell types [14]. The goal of this therapy is quite similar to surgical resection: lysing the entire tumor mass along with a 5-10 mm margin of surrounding normal tissue. The necrotic mass is then absorbed by the body over several months [15].

In order to achieve such high temperatures via transcranial, or non-invasive ultrasound, the frequency of the ultrasonic waves should be at least 650 kHz to reach deep-seated tumors (GBs, etc.) [16]. The thickness of the human skull, which is

about 6-9mm [17], causes significant attenuation of ultrasound. To account for such attenuation during thermal ablation, high powers up to 950 Watts are necessary for allowing acoustic waves to propagate through the skull. Unfortunately, this results in the skull absorbing the attenuated waves and an increase in temperature to dangerous levels, so several cooling down periods are required. An example of this is when Coluccia et al., performed the first non-invasive transcranial thermal ablation of GB [16]. The procedure lasted 5 hours with the patient awake lying in the supine position inside the magnetic resonance imaging (MRI) scanner. Long cool down breaks were required between short FUS exposures. Multiple points of ablation were visible in the tumor, but the entire tumor could not be ablated within this one treatment. Despite the advantages of a non-invasive procedure (i.e., closed skull, less risk of infection), the patient suffers due to a long and uncomfortable process that leaves parts of the tumor untreated.

Due to the disadvantages and complications of non-invasive thermal ablation, researchers are investigating minimally invasive HIFU procedures, where a small portion of the skull is removed, helping to eliminate the attenuation caused by the skull [18–20].

Enhanced Chemotherapy via BBB Opening

The BBB, while protective in many respects, often presents a blockade during chemotherapy drug delivery, especially in the case of GB. Although GBs commonly disrupt portions of the BBB, they are also highly vascularized and diffuse into healthy brain tissue that is still protected by the BBB. This results in significantly lower chemo-agent concentrations in the peritumoral tissue compared to the tumor center [21]. Fortunately, the BBB can be opened through various mechanisms: FUS, photochemical internalization, photodynamic therapy, etc. [22]. FUS has gained significant traction for this application due to its non-invasive characteristics. FUS has the ability

to locally and temporarily open the BBB when applied in combination with an injection of microbubbles. Available in various sizes, microbubbles typically consist of gas contained in a synthesized phospholipid shell [23]. After systemic injection, microbubbles circulating past the BBB will expand and contract when exposed to FUS, leading to cavitation effects. This cavitation applies pressure to the BBB, eventually opening a small portion to allow for temporary passage of drug-based treatments [22]. Depending on the ultrasound parameters, microbubbles may be destroyed by ultrasound or they will be cleared via the reticuloendothial system [24]. Mainprize et al. treated 5 patients with high-grade gliomas using chemotherapy in combination with FUS BBB opening. After receiving treatment, surgical resection was performed, in which sonicated and unsonicated regions of the tumor were collected and tested for chemo-agent concentrations. Of the 5 patients, 2 had quantifiable results showing an increase in chemo-agent concentrations in sonicated regions when compared to unsonicated regions [25]. This mechanism should be further studied to optimize parameters, chemotherapy session numbers, and chemotherapy doses.

Radiosensitization

Radiation therapy which uses high doses of radiation targeted at cancer cells to destroy their DNA can be more effective when used in combination with elevated temperatures, or hyperthermia. Prior to chemotherapy-aided BBB opening, as well as the discovery of TMZ, a chemo-agent that can cross the BBB, radiation was the primary source of GB treatment. Ways of sensitizing radiation therapy were heavily investigated and inducing hyperthermia during treatment was quite promising [26]. Unfortunately, this required invasive heat probes to be placed inside the brain during radiation therapy [26]. After advances in chemotherapy, radiosensitization using hyperthermia was abandoned. In light of the advancements made in the field of FUS, hyperthermia can be induced non-invasively. The hyperthermia level (41°C) [27] can

be achieved with transcranial FUS without overheating the patient's scalp since less power is required for this procedure. Hyperthermia in conjunction with radiation therapy increases perfusion and oxygenation in and around the tumor, which activates an immune response and causes cell death [26].

Sonodynamic Therapy

SDT requires the use of a sonosensitizer (i.e., a molecule that is sensitive to ultrasound). The leading research of this therapy focuses on GBs since 5-aminolevulinic acid (5-ALA) is preferentially taken up by these tumors and is converted to protoporphyrin IX (PpIX) within the cells, which serves as the sonosensitizer. GBs become highly vascularized by sprouting new capillaries from pre-existing vessels, significantly affecting the BBB within their region, which ultimately allows for GB uptake of 5-ALA [28]. Regardless of BBB passage, 5-ALA is preferential to GB cells, which is believed to occur due to selective uptake by an ATP-binding cassette transporter (ABCB6) which regulates porphyrin synthesis [29–31]. Once inside GB cells, 5-ALA is converted to fluorescent PpIX, which allows it to be regularly used in guided resection surgeries. There are eight enzymatic steps involved in heme synthesis between the mitochondria and cytoplasm, which include the transition of 5-ALA into PpIX [30]. CPgenIII is a product of the fifth enzyme, uroporphyrinogen III decarboxylase, and it enters the mitochondria from the cytoplasm to aid in the synthesis of PpIX [30]. This process is energy-dependent, so CPgenIII movement requires ABCB6. GB cells have been shown to possess significantly greater levels of ABCB6 than healthy cells [30–33]. The interaction between FUS and PpIX within GB cells causes the generation of reactive oxygen species (ROS), producing direct cytotoxic effects in the cells [34].

In an *in vitro* study by Sheehan et al., rat C6 and human U87 GB cells underwent SDT and responses were analyzed using a cell viability assay and apoptosis staining. Apoptosis staining showed a significant difference ($p < 0.05$) between the SDT groups

and control groups [35]. In an *in vivo* study by Wu et al., C6 GB rat models underwent SDT with single and multiple focal point treatment. Tumor volume over time and survival rate were monitored in all groups, resulting in a significant difference between the SDT groups and control groups (($p < 0.01$) for tumor volume, ($p < 0.01$) for survival rate), and even a significant difference in survival time between the single point and multiple point treatment groups ($p < 0.05$) [34]. Since 5-ALA is already regularly used in patients with GB and shows promise as a sonosensitizer, SDT should be further explored as a treatment for GB.

Immunomodulation

Immunotherapy, which refers to treatment of a disease by activating or suppressing the immune system, has long been investigated in the field of cancer research. The need for tumor-specific antigens is great when it comes to cancers that frequently recur (e.g. GB). FUS has the potential to induce such antigens that can cause an immune response which may help fight off recurrences. Prior to the surge in cancer research using FUS, Wissniowski et al. used radiofrequency ablation (RFA) to activate tumor-specific T lymphocytes in a VX2 hepatoma rabbit model [36]. Once activated, these tumor infiltrating lymphocytes were shown to recognize and kill cancer cells. Two weeks after RFA, there was a marked activation of peripheral T cells against tumor lysate in the treatment group while there was none in the control group. In addition, the liver bearing the tumor underwent immunohistochemical analysis and showed a massive increase of T-lymphocytes in and around the tumor for animals sacrificed at the end of the study compared to those sacrificed mid-way and those in the control group [36]. To further investigate the effects of activated antigens, den Brock et al. used RFA in a mouse model to promote tumor antigens arising from melanoma and tested their validity by reintroducing the cancer later on [37]. In this study, RFA was used to destroy most of the tumor volume, so the survival rate was very high. After

a long survival period was observed, mice were re-injected with melanoma cells to investigate immune response. Thirty days after cancer cell reintroduction, no mice in the control group were living, while 80% of immunotherapy-receiving mice were still surviving [37].

This antitumor immunity effect gave promise to the possibility of collecting debris resulting from ablation to create a tumor-specific vaccine that could be utilized to treat first-time cancerous animals. Zhang et al. presented a study in which there was an increase in cytotoxicity as well as a decrease in tumor volume for mice treated with a debris vaccine, but these results were enhanced in mice that were treated with HIFU originally and then re-challenged, indicating that an *in situ* vaccine specific to the individual shows most promise for recurring types of cancer (e.g. GB) [38]. If ablation/hyperthermia is the main cause of this immune response, this would present an issue in GB treatment, as HIFU through the skull has already been proven to be a challenge. Fortunately, additional studies have shown that this may not be the case. Hu et al. explored the release of exogenous danger signals from thermal and mechanical HIFU-treated tumor cells and how they stimulate antigen-presenting cells (APCs) [39]. HIFU performed with parameters eliciting mechanical lysis of tumor cells primarily caused the release of a danger signal known as heat shock protein 60 (hsp60). The release of this signal was five times greater for mechanical HIFU than thermal HIFU. HIFU performed with parameters eliciting thermal necrosis of tumor cells primarily caused the release of the danger signal, ATP, but the release was stable throughout and did not progress as treatment continued. In addition, the maturation of APCs was much more evident in mechanical HIFU than thermal HIFU. This shows promise that FUS-induced immune response of cancer cells can be used as a prevention for recurrence of GB.

Focused Ultrasound Therapies for GB

From this review, it is evident that there are numerous FUS therapies with the potential to treat GB. More research needs to be conducted for each therapy, and this thesis will explore devices that can be used for most, if not all of them.

Chapter 2

Minimally Invasive Focused Ultrasound Device for Neurosurgery

Introduction

FUS is a growing technique for both noninvasive and minimally invasive surgical (MIS) procedures, especially in neurosurgery[1]. It is most helpful for inoperable brain lesions, as it can thermally ablate tissue from a distance when used at high intensities. GBs are the most common malignant primary brain tumors, accounting for 50% of malignant primary brain tumors [40]. GBs infiltrate healthy tissues and are therefore difficult to surgically remove [11]. MIS FUS has the potential to lyse remaining tumor tissue after resection, or more optimally - ablate the bulk of the tumor without having to remove as much of the skull when compared to traditional resection surgeries. Noninvasive ultrasound can also be used to treat brain lesions, but there are several limitations such as the attenuation of ultrasound through the skull. To overcome this issue, high power is required, which can result in the transducer overheating when in contact with the patient's scalp. As a result, researchers are investigating MIS

[1]The work in this chapter is reproduced from: M. Acord, T. P. Kaovasia, N. J. Gamo, T. Xiong, E. Curry, F. Aghabaglou, K. Morri-son, B. Tyler, M. Luciano, and A. Manbachi, "Design and Fabrication of a FocusedUltrasound Device for Minimally-Invasive Neurosurgery: Reporting a Second, Minia-turized and MR-Compatible Prototype with Steering Capabilities," *American Society of Mechanical Engineers*, vol. 2021 Design of Medical Devices Conference, 2021.

FUS procedures, where a small portion of the skull is removed, helping to eliminate the attenuation caused by the skull [18–20]. However, there is much debate on how "minimally invasive" the procedures should be.

As described in a previous study by our group [18], an ultrasound-guided focused ultrasound (USgFUS) probe was designed with a 9mm x 32mm curved transducer with a housing diameter ranging from 12mm-15mm to include the imaging transducer. The first transducer design was abandoned due to lateral mode effects, which led to issues with the transducer overheating. That transducer design was replaced with three circular, 8mm diameter transducers, still fitting in the same housing (Design II reported in [18]). This probe was envisioned to fit inside common MIS technology, such as BrainPath (NICO Corporation, Indianapolis, IN), which is a trocar device that allows atraumatic access to the brain. The largest BrainPath device, which was 13.5mm in diameter [41], was able to house the FUS transducer portion of the probe, but not the imaging transducer portion (see Fig. 2-1).

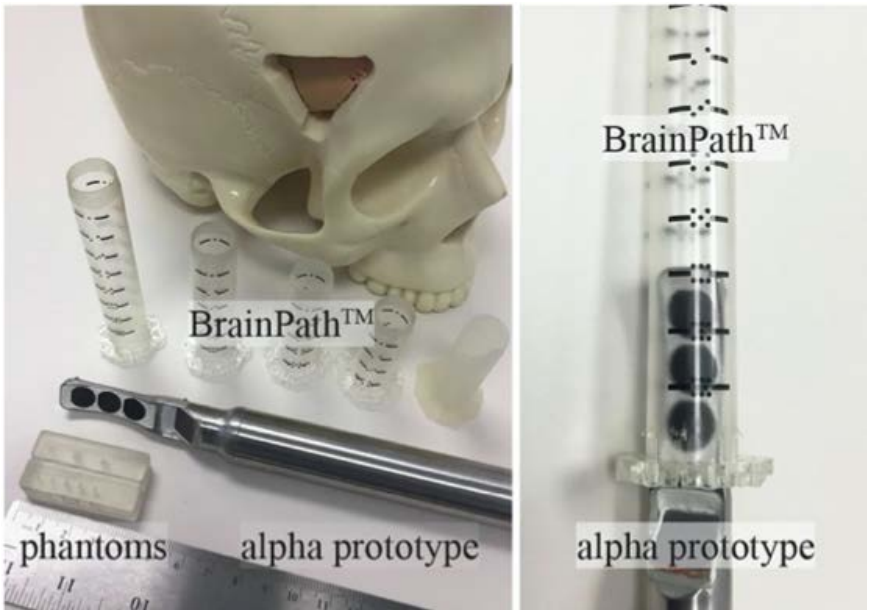

Figure 2-1. First Generation HIFU Probe: BrainPath is a Minimally Invasive Neurosurgical Toolkit, Envisioned to Host this Focused Ultrasound Device (reproduced with permission from [18])

This led to the second-generation probe (see Fig. 2-2), which will be contained within a 10mm diameter housing, which fits within the 11mm diameter BrainPath trocar, allowing the device to be used for MIS. In addition to size reduction, this new design has electronic steering in the axial direction, enabling the user to reach lesions at various distances from the probe within the brain, without manual movement of the probe. Lastly, the new prototype is designed to be MR-compatible, in order to provide ease-of-use to clinicians, who may be trained for MR-guided procedures, and may find ultrasound image-guidance difficult to interpret during an involved surgery.

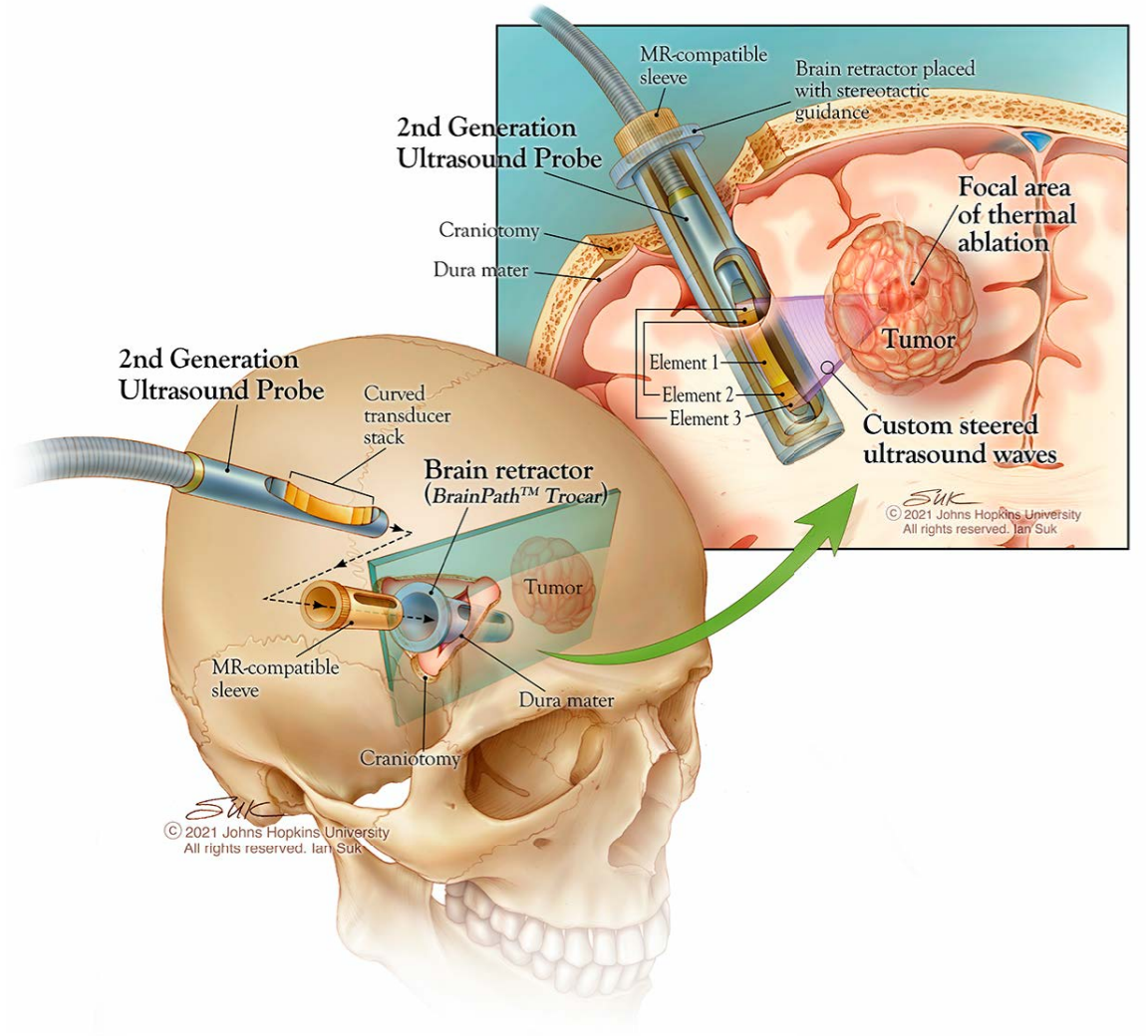

Figure 2-2. Minimally Invasive High Intensity Focused Ultrasound Procedure Schematic, *Medical Illustration by Ian Suk.*

Materials and Methods

Design and Fabrication

The advantages of reducing the size of the probe are two-fold: the procedure is less invasive and the full probe can fit into the BrainPath trocar. The first goal of the second-generation probe design was to create an MR-compatible probe that can be used in procedures requiring MRI guidance. Designed and fabricated by Sonic Concepts Inc. (Bothell, WA), the H-284 model is an MR-safe, 1.2MHz HIFU transducer with +/- 50% bandwidth. The transducer is contained in plastic housing as seen in Fig. 2-3, making the entire probe MR-compatible.

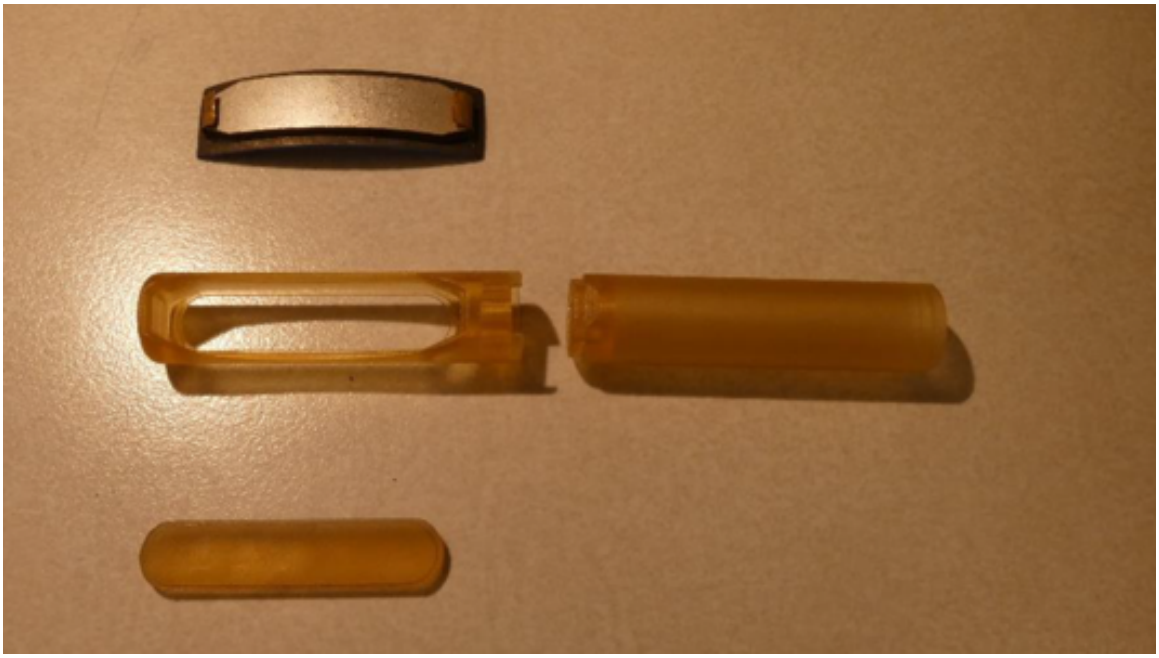

Figure 2-3. Transducer Stack and MR-Safe Housing (reproduced with permission from [42])

In terms of size, the transducer has a 45mm radius of curvature (ROC) with a total 7mm x 32mm rectangular aperture (see Fig. 2-4). Piezo-composite pillars (see Fig. 2-5) are hypothesized to reduce the lateral mode effects seen in the first-generation probe Design I. This new approach should provide optimal performance without overheating the transducer.

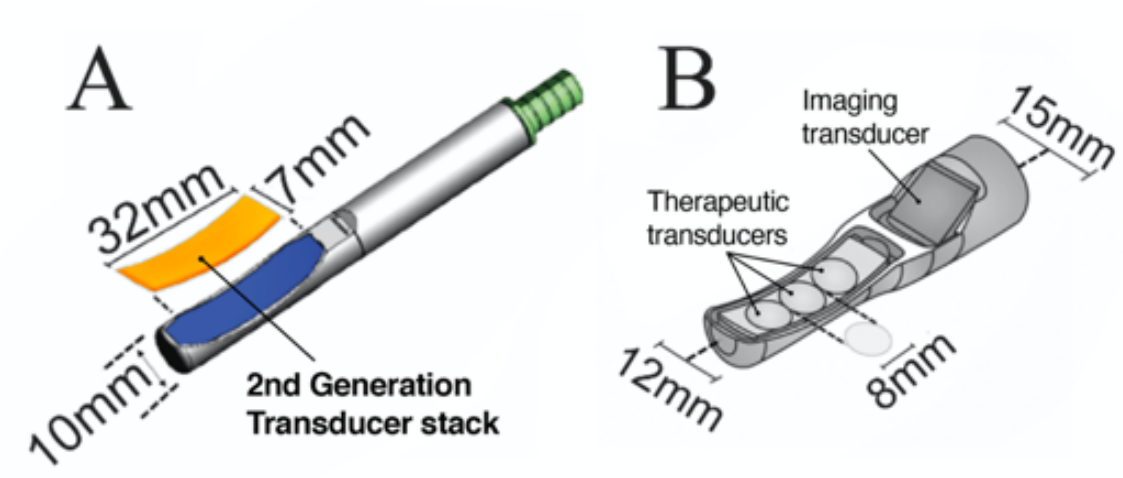

Figure 2-4. (A) Second Generation and (B) First Generation Probe Designs (reproduced with permission from [42])

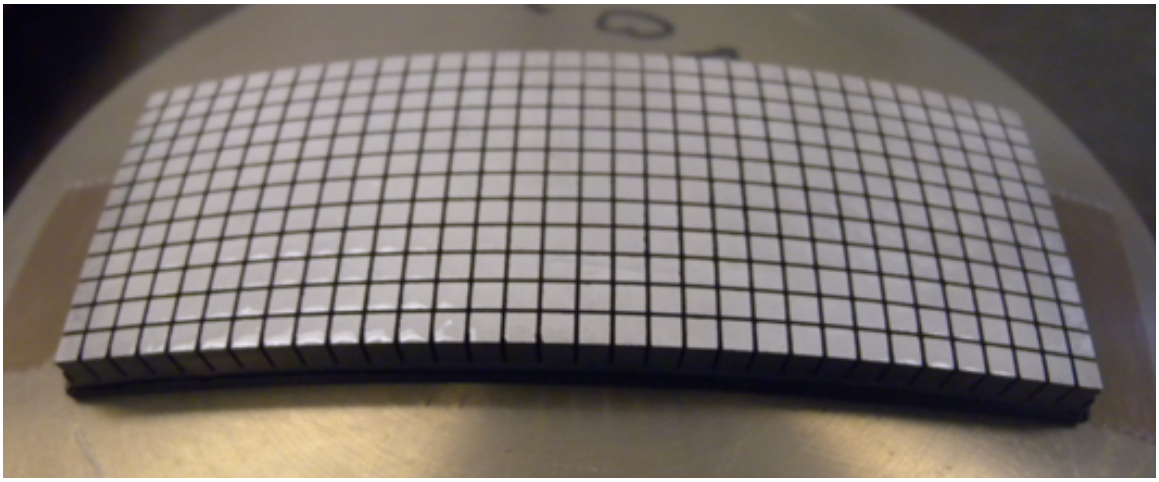

Figure 2-5. Piezo-Composite Pillars Used to Reduce Lateral Mode Effects (reproduced with permission from [42])

The other main improvement of the second-generation probe is its focal point steering capability. The focal point can be electronically steered along the axial dimension through the use of time delays in the activation of different array elements, which results in phase differences between the array elements. The total aperture of this transducer is divided into three elements (see Fig. 2-6).

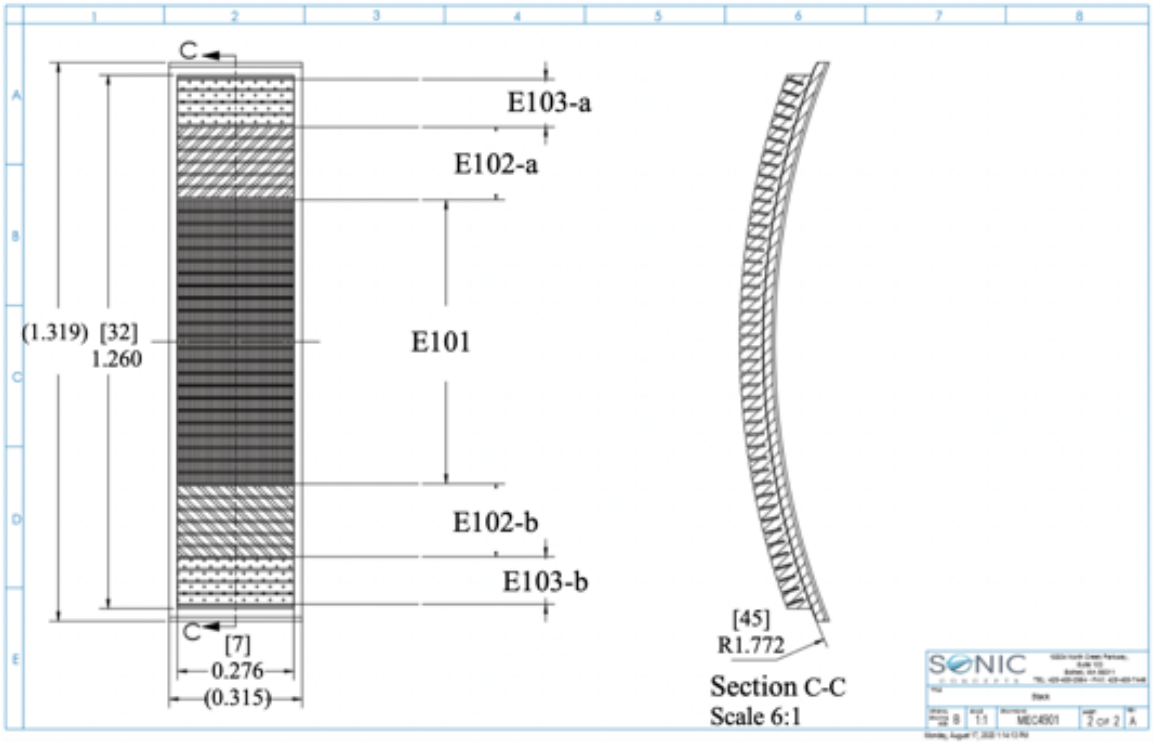

Figure 2-6. Second Generation Transducer Design with Three Elements Allowing for Electronic Steering (reproduced with permission from [42])

PiezoCAD Simulations

FUS transducers are electronically interfaced to a signal generator and power source. To ensure maximum power transfer between the source and the transducer (as well as its subsequent conversion to acoustic power), both impedances should be the same [43]. Therefore, an impedance-matching circuit is used. Commercially available sources operate at an equivalent (Thevenin) output impedance of 50 Ω, which means the transducer should be matched to have an input impedance of 50 Ω [44].

To ensure that the transducer would be designed in such a way as to possess an impedance of 50 Ω, PiezoCAD simulations were utilized to model the transducer. The transducer consists of a piezoelectric crystal, with both ends of the crystal coated in a conductive material such as sputtered chromium-gold. With this design, the transducer behaves like a capacitor whose impedance is frequency-dependent. The

crystal converts electrical pulses to acoustic waves and is designed to operate around a central frequency [45]. This frequency affects the electrical impedance of the transducer, which in turn affects the transmitted and converted power. The PiezoCAD software, designed by Sonic Concepts, was used to study the effect of varying the frequency on the magnitude and associated phase angle of transducer impedance, as well as the transmitted transfer function (ratio of the acoustic output power to the electric power provided by the source) for each element [46]. These effects were also investigated for a parallel combination of all three elements.

The parameters and subsequent values of the electrical matching network for each of these four cases are listed in Table 2-I. The series inductance (L) and resistance (R), shunt inductance (L), and transformer serve as the circuit to match the impedance of the source to that of the load (transducer elements). The inductive reactance (XL) varies with frequency (f): XL= j2πfL. Therefore, the resistance and inductance values are selected to match the impedance at the center frequency. The coaxial cable connects the source to the transducer elements. For maximum power to be transferred over the cable, from the source to load, the impedance of this cable should match that of the source and load (50 Ω).

Table 2-I. PiezoCAD Simulation Parameters (reproduced with permission from [42])

Transducer Element	Parameter	Value
Element 1	Series L	10 μH
	Series R	1 Ω
	Coaxial Cable	50 Ω, 2 m, 28 dB/km at 1MHz
	Shunt L	66.31 μH
	Transformers	1:3.84 turns
Element 2	Series L	10 μH
	Series R	1 Ω
	Coaxial Cable	50 Ω, 2 m, 28 dB/km at 1MHz
	Shunt L	66.31 μH
	Transformers	1:3.84 turns
Element 3	Series L	10 μH
	Series R	1 Ω
	Coaxial Cable	50 Ω, 2 m, 28 dB/km at 1MHz
	Shunt L	53 μH
	Transformers	1:2.2 turns
Elements in Parallel	Series L	10 μH
	Series R	1 Ω
	Coaxial Cable	50 Ω, 2 m, 28 dB/km at 1MHz
	Shunt L	110 μH
	Transformers	1:1.58 turns

Field II Ultrasound Simulations

To gain an understanding of the focusing and steering capabilities for this transducer, ultrasound fields showing focal point location and pressure were simulated using the Field II Ultrasound Simulation Program [47]. The program uses the Tupholme-Stepanishen method, which can be used to calculate pulsed, continuous-wave, and pulse-echo ultrasound fields. The calculation is done by dividing the surface into small rectangles and summing their response [48].

The purpose of this simulation was to determine the phase angle limits, and thus, the focal point location limits. The multi-element transducer presented here allows for phase (or time) delays, measured in radians, between the elements which will shift the focal point to different distances away from the probe. Various phase delays

were simulated to examine the furthest and closest possible focal point locations without having any unwanted effects, such as grating lobes, which result from energy that spreads out from the transducer at angles other than the primary path. This will help determine the depths in the brain at which lesions could potentially be treated. It is important to note that these simulations are done in a homogenous medium, such as blood or water, and hence will not be fully representative of the non-homogenous tissues of the white and gray matter. Despite this assumption, the results of these simulations can provide a general understanding of the focusing and steering capabilities of the new transducer design.

Results and Discussion

PiezoCAD Simulations

Due to the capacitive nature of the transducer, its impedance depends on the frequency of the electrical signal. Fig. 2-7A shows the variation of both the magnitude and phase angle of the impedance with frequency. The red line shows the impedance (50 Ω with a phase angle of zero) of the transducer at its center frequency (1.2MHz).

As the impedance of the transducer varies, its impedance can get mismatched with the power source. Due to this mismatch, the transfer function may decrease; however, the impedance and the corresponding transfer function at the operating center frequency were the sole focus of this analysis. Figs. 2-7B, 2-8, 2-9, and 2-10 show the variation of the transfer function with frequency, with the red line passing through the center frequency.

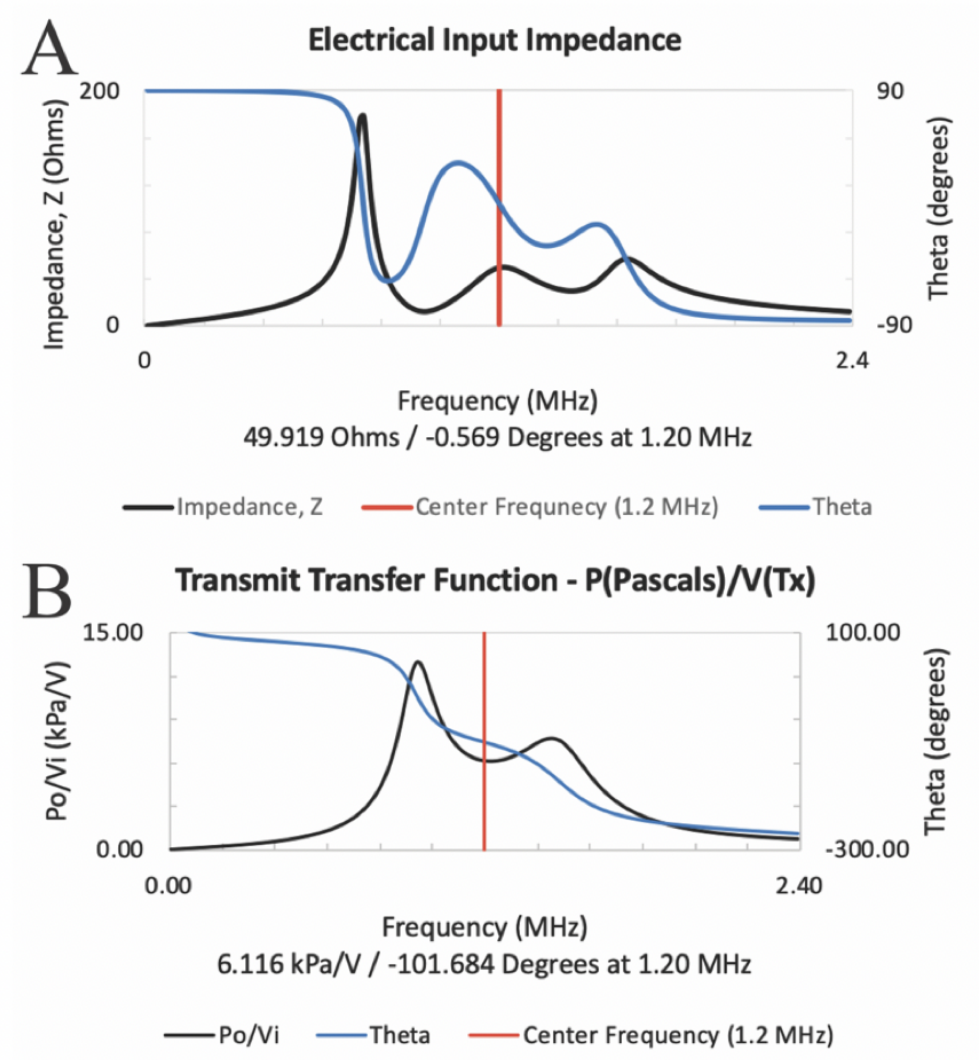

Figure 2-7. (A) Impedance Curve for Element 3. (B) Transmitted Transfer Function Curve for Element 3 (reproduced with permission from [42])

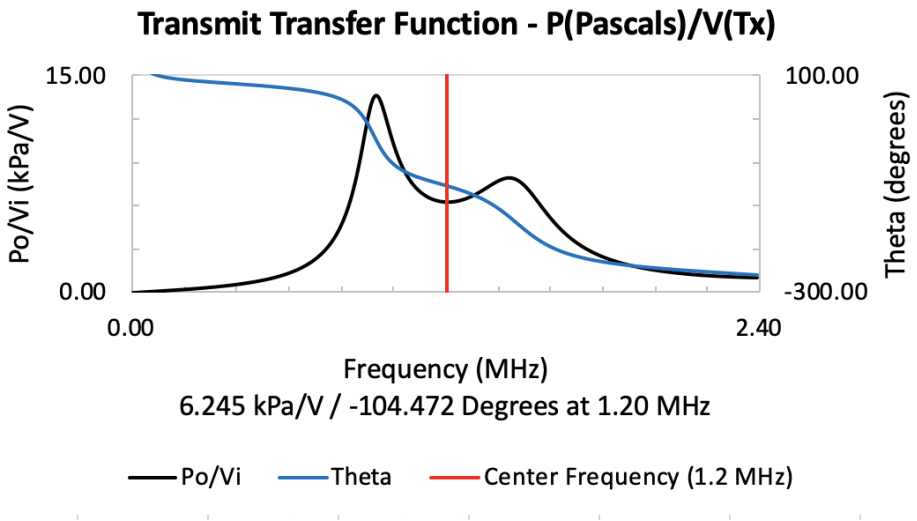

Figure 2-8. Transmitted Transfer Function Curve for Element 2 (reproduced with permission from [42])

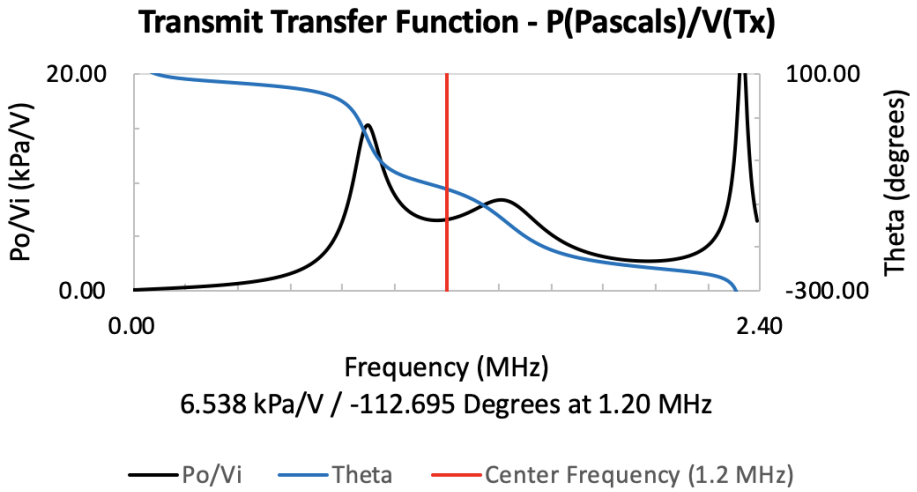

Figure 2-9. Transmitted Transfer Function Curve for Element 1 (reproduced with permission from [42])

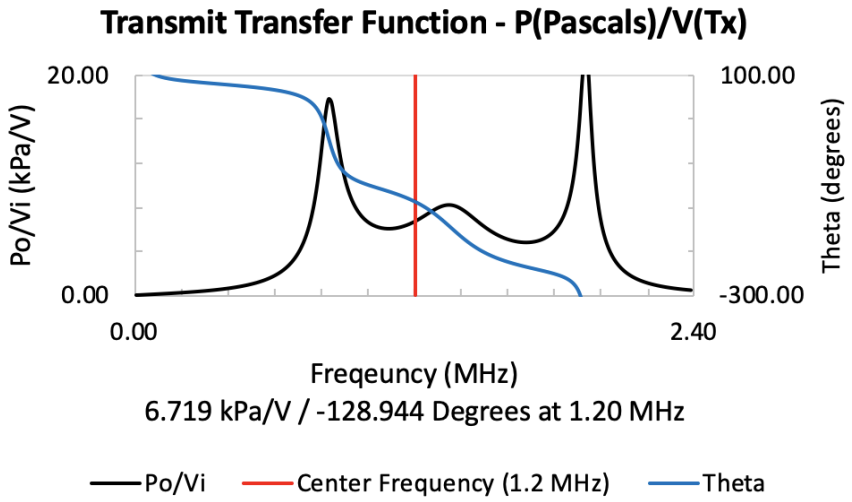

Figure 2-10. Transmitted Transfer Function Curve for all Elements in Parallel (reproduced with permission from [42])

Table 2-II shows the magnitude and phase angle of the impedance for element 3 and the transfer function for elements 1, 2, 3, as well as the parallel combination of them at center frequency. Consistency in the magnitude and phase of the transfer function were seen in each case, which demonstrates the reliable operation of the probe.

Table 2-II. PiezoCAD Simulation Results

Transducer Element	Parameter	Value
Element 1	Impedance	49.919 Ω | -0.569°
	Transmitted Transfer Function	6.116 kPa/V | 101.684 °
Element 2	Transmitted Transfer Function	6.245 kPa/V | 104.472°
Element 3	Transmitted Transfer Function	6.538 kPa/V | 112.695°
Elements in Parallel	Transmitted Transfer Function	6.719 kPa/V | 128.944°

Field II Ultrasound Simulations

There is a great need for electronic steering of the focal point when treating brain tumors, the dimensions of which are within the centimeter range. The focal point may be 2-5 mm in length, but unfortunately, GB tumors may have a cross-sectional

area of 1100 mm^2 [49]. For HIFU to be effective and remain minimally invasive, the probe must have the capability to move the focal point to treat larger tumors. A transducer of this size and curvature will create a focal point about 4.1-4.5 cm away. By changing the phase angle, and thus, creating time differences in the firing order of the three elements, the focal point can be moved closer or farther from the transducer. Various angles were tested, and acceptable limits were found to be -2.25 radians and 0.75 radians. Table 2-III shows these angles and their respective location information.

Table 2-III. (Acceptable Phase Angle Limits and Their Respective Focal Point Locations reproduced with permission from [42])

Phase Difference (in radians)	-2.25	0	0.75
Phase Difference (in degrees)	-128.9°	0°	49.9°
Zmax	33	42	46

Figs. 2-11 and 2-12 show two different perspectives of the focal point simulations for each phase angle. Here, grating lobes were shown to start appearing on the limiting phase angles. One can see that no phase angle produced a clear, straight, non-deviating energy path toward the focal point. However, the other limiting phase angles produced grating lobes that could result in unwanted and potentially harmful high-pressure points before the focal point. Employing phase angles outside of these limits could cause extra focal points to be created in healthy tissue, which could be harmful.

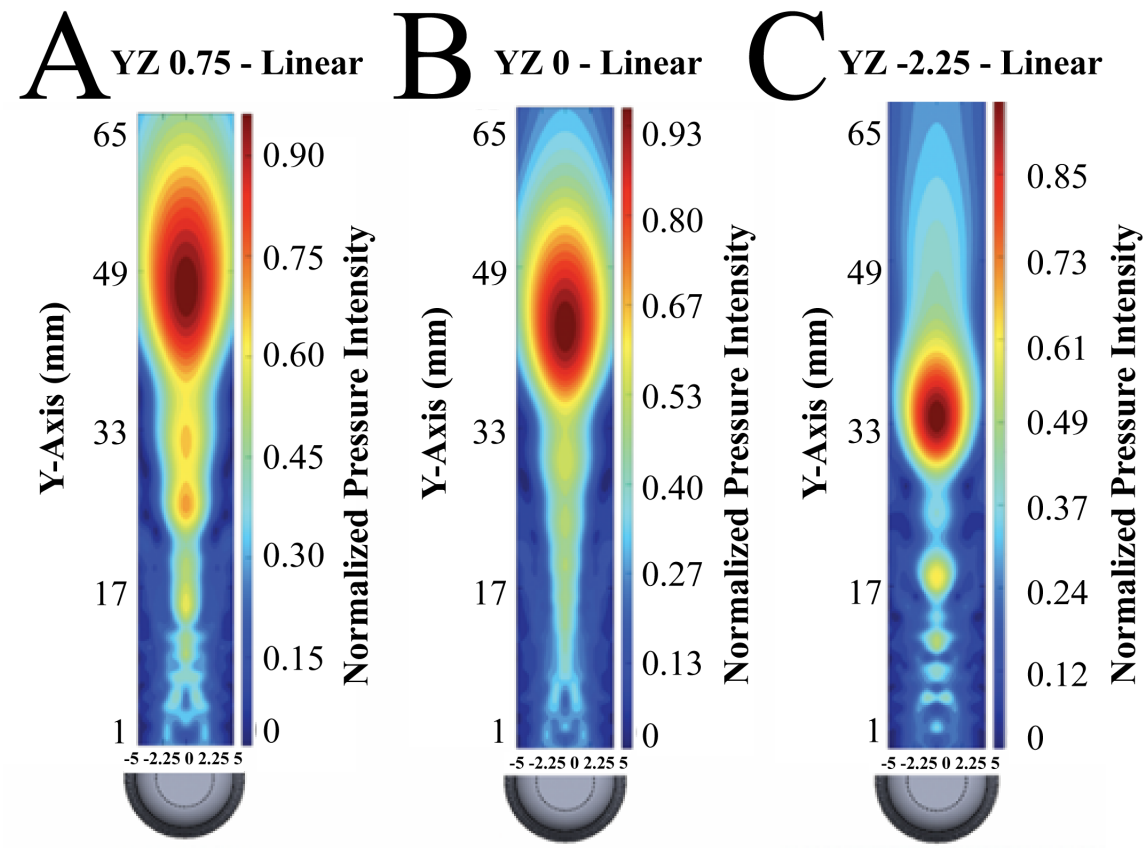

Figure 2-11. (A) Focal Point Profile (YZ View) for a Phase Angle of 0.75 Radians, (B) Focal Point Profile (YZ View) for a Phase Angle of 0 Radians, and (C) Focal Point Profile (YZ View) for a Phase Angle of -2.25 Radians (reproduced with permission from [42])

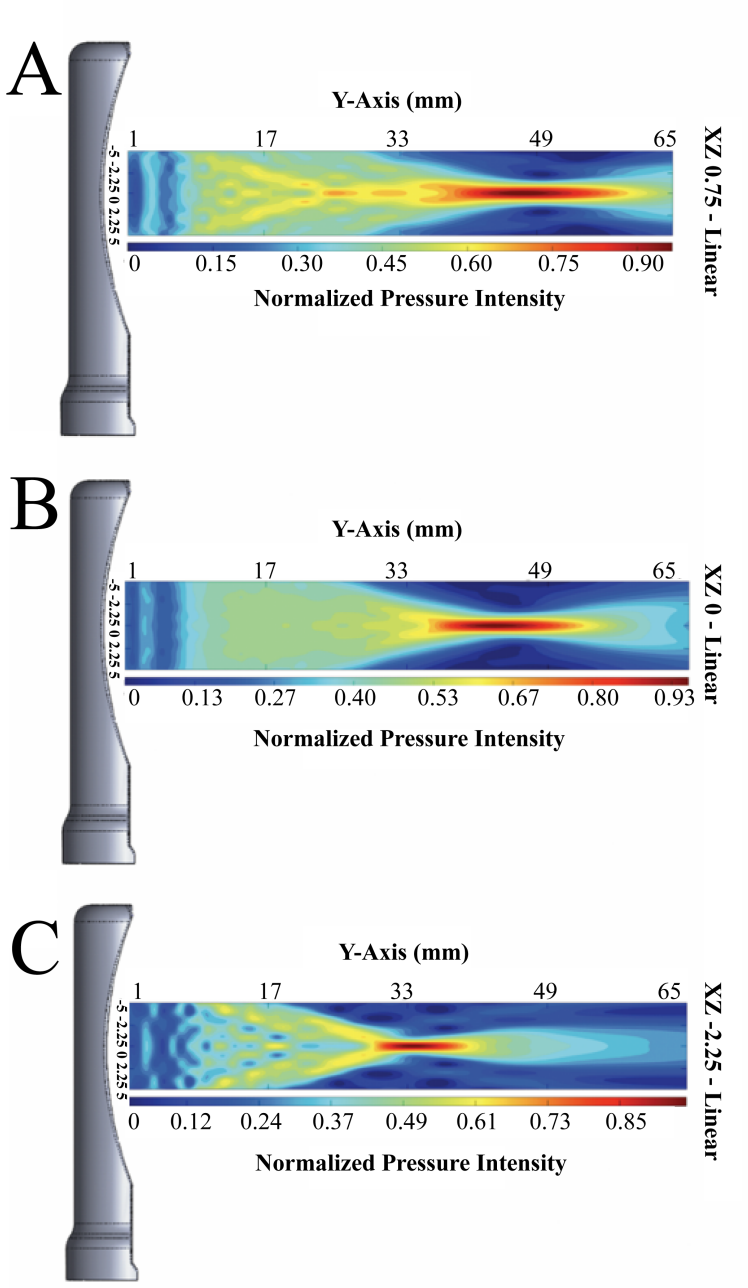

Figure 2-12. (A) Focal Point Profile (XZ View) for a Phase Angle of 0.75 Radians, (B) Focal Point Profile (XZ View) for a Phase Angle of 0 Radians, and (C) Focal Point Profile (XZ View) for a Phase Angle of -2.25 Radians (reproduced with permission from [42])

Potential Risks

With any brain surgery, minimally-invasive or noninvasive, there are always potential risks. The probe user should always inspect the transducer face and bonding for any damage before performing surgery, as damage to these may pose an electrical shock hazard. The surgeon should never submerge the probe past the handle, as the cord extending from the probe is not meant for invasive procedures. When performing MIS, surgeons have to perform a craniotomy or burr hole. Fortunately, they only need to remove a small portion of the skull the size of the BrainPath trocar, contrary to typical resection surgeries. Though this is still invasive, the need for thermal ablation can outweigh the risks for treating certain lesions like brain tumors. Without a craniotomy, there is far too much ultrasound attenuation through the skull, resulting in overheating and possible danger to the patient [18].

Conclusion

In this study, the design and fabrication of a FUS device were described in such a way that allows for miniaturization, steering of the focal point, and MR-compatibility. The first-generation design consisted of three circular, 8mm diameter transducers, fitting into a 12mm diameter housing, along with an adjacent imaging transducer, which extended the housing diameter to 15mm. The therapeutic transducers in the first-generation design were capable of fitting into a BrainPath trocar with a 13.5mm diameter, but the imaging transducer was unable to fit within the trocar. The second-generation transducer, discussed here, consisted of a 7mm x 32mm curved transducer, that fit into a 10mm housing. This probe is capable of fitting into a BrainPath trocar with an 11mm in diameter. Three elements were incorporated into the therapeutic transducer that allows for axial steering when time delays are introduced. The focus can be positioned approximately 4.1-4.5cm away from the transducer. This probe was

also designed to be MR-compatible, affording surgeons the ability to use the device with MRI guidance. The miniaturization enables MIS approaches for the treatment of brain lesions, while the steering capabilities of the focal point allow for the treatment of lesions of various sizes. MR-compatibility would pave the path for FUS treatments under MR-guidance. The MIS technique has the potential to allow for effective thermal ablation of GB in one procedure.

Chapter 3

RK-300: Magnetic Resonance guided Focused Ultrasound System

Introduction

System Basics

The RK-300 developed by FUS Instruments (Toronto, Canada) is a small animal research FUS device [50]. It is compatible with all Bruker Biospec horizontal bore MRI systems ranging from 3 to 9.4 Tesla. With its non-magnetic motors, the RK-300 is capable of 2-axis positioning allowing the user to select a sonication target anywhere within the 2D plane. The calibrated FUS transducer works for two frequencies: 1.106 MHz and 3.164 MHz. Sonications can be continuous-wave, pulsed-wave, and even planned and performed in a serial fashion. The image-based treatment planning software allows for registration of the focus and knowledge of the exact focus location within the animal or phantom being treated.

Potential Applications

The RK-300 has a number of potential applications that could be used for GB research, such as thermal ablation, non-invasive hyperthermia, BBB opening, SDT, etc. An early prototype of this system was used in a study mentioned previously, where C6 GB rat models were used to study the effects of SDT [34].

Phantom Study Overview

Given the numerous potential applications of the RK-300, it was important to test and confirm its primary functions: focus generation, focal point planning, and MR-guidance. A phantom study was designed to optimize focus finding, sample preparation, target planning, and real time MR imaging of water movement resulting from focus formation in the phantom.

Materials and Methods

Hardware, Software, and Components

The hardware shown in Fig. 3-1 consists of front-end electronics (i.e., the MR-safe arm which houses the transducer and mechanical motors) and back-end electronics (i.e., the controller and processor, function generator, power source, and RF power amplifier). The software shown in Fig. 3-2 can be accessed through the computer provided and serves as a user interface (UI) that allows for focus finding and treatment planning. There are several additional components that serve as tools for varying applications of the system. The primary components used in this study are shown in Fig. 3-3: the plastic sledge that covers the transducer section of the arm, the membrane cuboid that provides a sonolucent barrier between the water and sample, the additional water bath, and focal marker for focus finding.

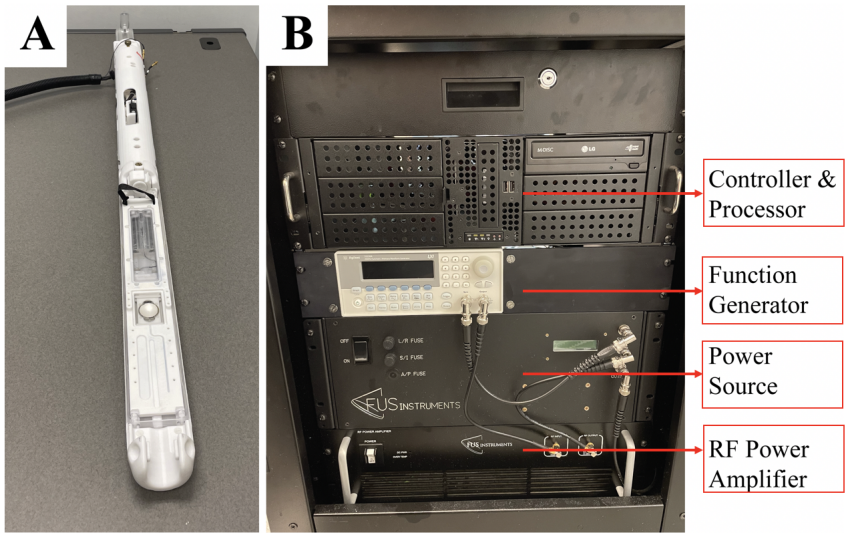

Figure 3-1. Front-end and Back-end Electronics. (A) MR-Safe arm housing transducer and motors. (B) Controller and Processor, Function Generator, Power Source, and RF Power Amplifier.

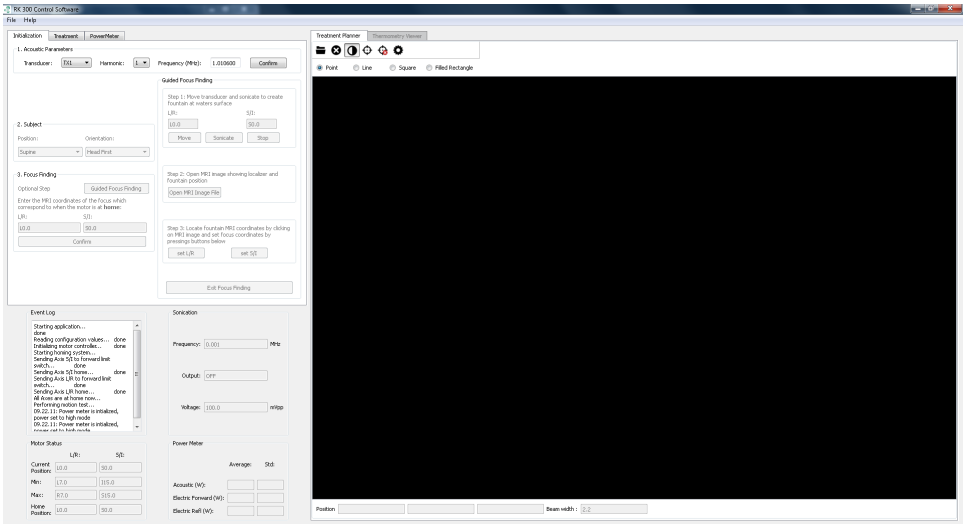

Figure 3-2. RK-300 Software User Interface

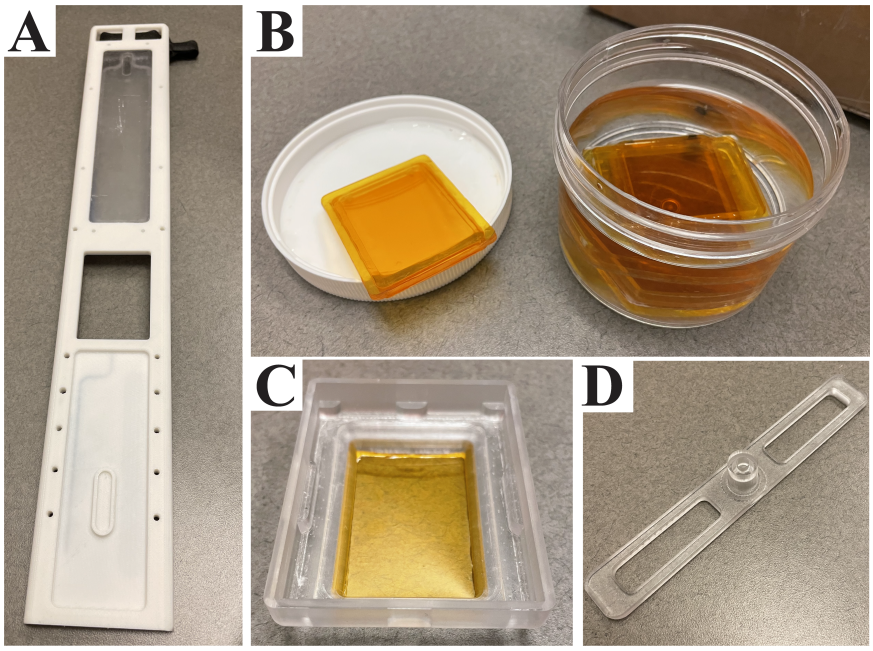

Figure 3-3. Components. (A) Plastic Sledge, (B) Membrane Cuboid, (C) Water Bath, (D) Focal Marker.

Registering the Focus

The space around the transducer was filled with degassed water and the plastic sledge was placed over the transducer section of the arm. Next, the membrane cuboid was placed over the transducer and water, ensuring no air bubbles. A small amount of water was deposited over the membrane cuboid and the water bath was placed on top, again ensuring no air bubbles. The bath was then partially filled with water for the guided focus finding. Within the initialization tab of the software, there is a "Guided Focus Finding" section that allows for sonication at 1 Watt in order for the user to see the transducer produce a focus creating a fountain in the water bath. By raising or lowering the water level in the water bath, the fountain can be sharpened. After the fountain was as sharp as possible, the focal marker was placed over the bath with the fountain at the center of the column. The marker was then taped down and the water bath filled almost completely. Next, the arm was placed into the MRI for T1 weighted FLASH scans. The resultant coronal scans were transferred to the RK-300

software in order to set the transducer position to home (0, 0, 0).

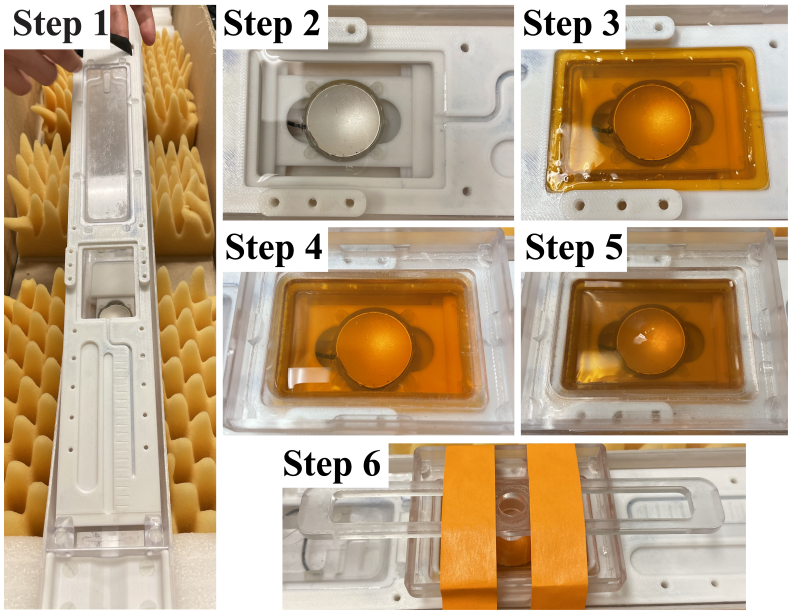

Figure 3-4. Focus Finding. (Step 1) Place plastic sledge over transducer section of the arm. (Step 2) Fill transducer cavity with degassed water. (Step 3) Place membrane cuboid over the transducer. (Step 4) Place water bath over membrane cuboid and add water. (Step 5) Sonicate and raise/lower the water level to sharpen fountain. (Step 6) Place focal marker.

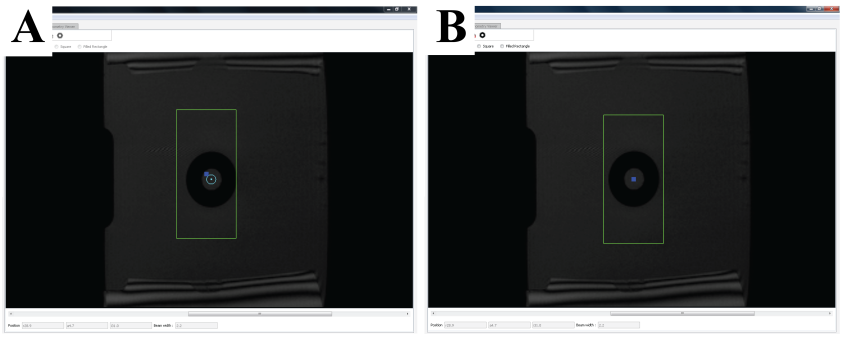

Figure 3-5. Focus Registration. (A) Setting the focus to the center of the column. (B) Focus set to center of column.

The Phantom

The phantom used in this study was a white solid-water tissue-mimicking phantom (CIRS, Norfolk, VA). The phantom was initially prepared by removing the water bath, depositing a layer of degassed ultrasound gel over the membrane cuboid, and securing

the phantom to the membrane. Unfortunately, this led to bubbles formed when the gel folded into itself. Bubbles were resolved by replacing the water bath and adding the phantom in water (see Fig. 3-6). The RK-300 arm with phantom secured was then returned to the MRI for T1 weighted FLASH scans (see Fig. 3-7).

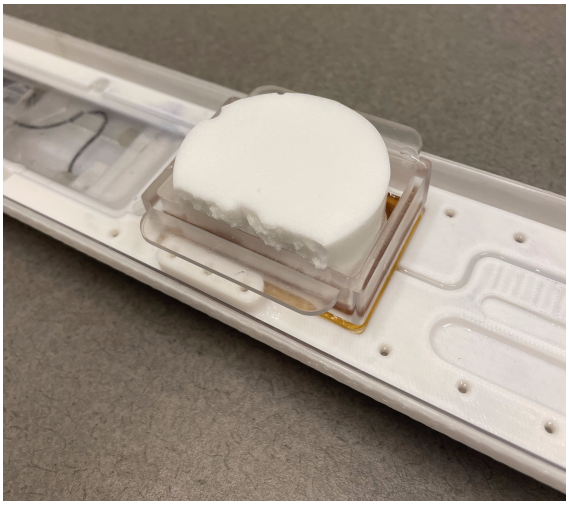

Figure 3-6. Solid-water tissue-mimicking phantom from CIRS, Norfold, VA.

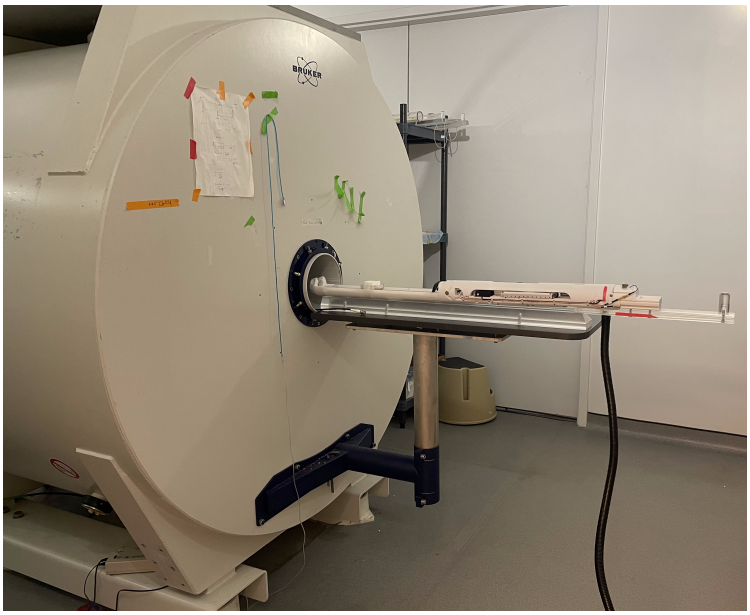

Figure 3-7. The RK-300 is designed to slide securely and safely into an MRI with butterfly adapter.

Selecting a Target

Initially, the coronal scans were transferred to the RK-300 software for focal plane determination. The middle coronal slice (showing the middle of the transducer) was selected. Following the Pythagorean theorem (see Fig. 3-8A), the focal plane was calculated. The height of the focal plane (15.61mm) was subtracted from the blue focus point's corresponding p-value, found at the bottom of the window in light blue, to determine the slice value (p-value) of the axial view. Axial scans were then transferred to the software and the correct focal point slice was used for sonication target planning (see Fig. 3-8B). The focus could be moved to a desired location in the fixed z plane, as shown in Fig. 3-8C.

Sonication

In order to generate a focus that could be viewed with real-time MRI, 2 Watts of power were used with a frequency of 1.106 MHz for continuous sonication. The sonication time was set to 15 seconds and the wait time was set to 10 seconds. 15 T1 weighted FLASH scans of the axial slice being sonicated were taken in sequence to capture the water movement created by focus generation. Each image was acquired over 5 seconds. Two images were acquired and then sonication began for 15 seconds, capturing about 3 images during this time.

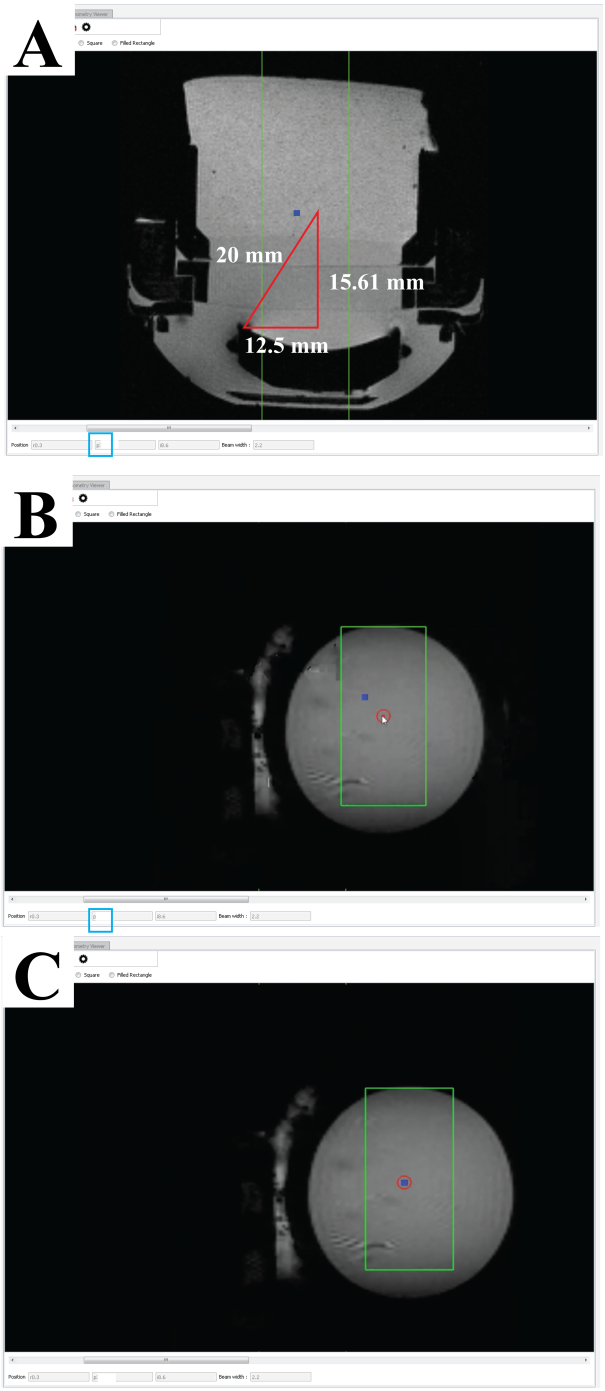

Figure 3-8. Target Selection. (A) Finding the correct focal plane in the axial view and corresponding slice number. (B) Corresponding coronal slice. (C) Selecting the desired target in the coronal plane.

Results and Discussion

T1 weighted FLASH single slice scans acquired during sonication revealed a focus generation (see Fig. 3-9). The phantom began at the hyper-intense/hypo-intense interface with the phantom being hypo-intense. The focus (hyper-intense cone) did not go into the phantom as expected. This was likely due to the phantom partially floating in the water bath rather than being flush with its bottom surface. The light gray line that cuts the middle of the cone was the membrane cuboid. It was understood that the focus was fully formed due to the approximate width and height of the focus ellipsoid measured during post-processing. The width and height of the focal spot according to FUS Instruments specifications were 1.7 mm and 9.3 mm, respectively. Post-processing measurements of the narrowest width and shortest height were found to be 2.52 mm and 10.14 mm, respectively, indicating the focus was fully formed below the phantom. In the next study, the phantom should be pressed down securely and kept flush with the bottom of the water bath.

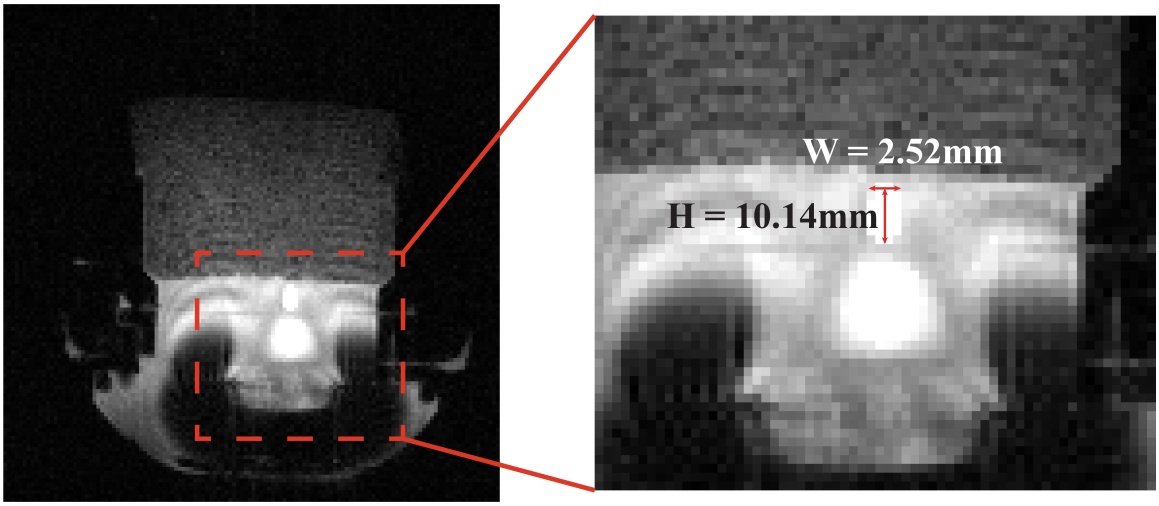

Figure 3-9. MRI Scan of focus generation during sonication.

Conclusion

Through this phantom study, functionality of the RK-300 was confirmed. The guided focus finding procedure allowed for the focus to be registered at the home position. Treatment planning was successful in that the x,y planes selected for sonication corresponded to the correct axial slice used for real-time MRI. A clear focal point of appropriate size, defined by the manufacturer, was visible with real-time MRI.

Chapter 4

Fiber Optic Temperature Sensing During Focused Ultrasound Procedures

Introduction

Focused Ultrasound in the Brain: The Unknowns

FUS in the brain is only FDA approved for the treatment of essential tremor [51]. Part of this is due to the unknown effects of the technology and the lack of ability to monitor certain biomarkers during treatment. A major concern for HIFU treatments in the brain is temperature change. MR thermometry is currently what is used to track temperature changes, but this is not a real-time measurement. FLASH gradient echo sequences can be used for capturing real-time images and temperature maps are then processed after imaging [34], delaying the temperature information. If any type of craniotomy is performed, such as for MIS, temperature probes could be used for real-time monitoring, but this adds a more invasive component to the already invasive procedure. Therefore, in order to incorporate HIFU into standard clinical treatment, there is great need for a minimal to non-invasive real-time temperature monitoring method that can be used during FUS therapies in the brain.

Fiber Optics

Optical fibers are thin, flexible, transparent glass fibers that transmit light from one end of the fiber to the other. They are typically comprised of a core with a high refractive index and surrounded by transparent cladding with a lower refractive index. Light particles (photons) remain trapped inside the core and travel along the fiber due to the phenomenon of total internal reflection (TIR). TIR occurs when photons in one medium strike the boundary in an oblique fashion with a second external medium, in which light travels faster than in the first internal medium.

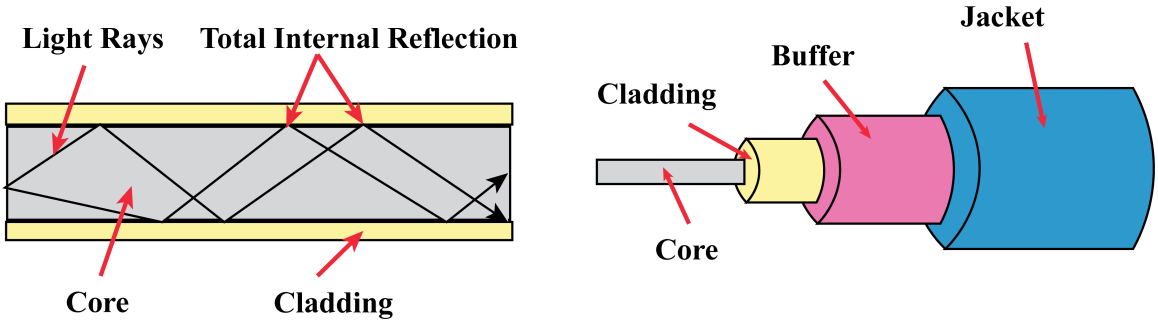

Figure 4-1. Principles of fiber optics. Light remains trapped in the core and travels along the fiber due to TIR.

Fiber optic temperature sensors operate on the principle based on the temperature dependence band gap of gallium arsenide (GaAS) crystal. The crystal is fixed on the sensing tip of the fiber and behaves as a temperature sensitive filter, where the crystal absorbs light at certain wavelengths and reflects light at other wavelengths depending on the temperature of the medium it's in. The light reflected back is sent to a miniature spectrometer, which provides a spectrum based on the temperature [52]. More specifically, the system is recording the photo energy that is sufficient enough to excite an electron from the valence band to the conduction band of the crystal. That required amount of energy is referred to as the band-gap energy. The transition wavelength that separates the absorbed and reflected wavelengths is determined by the crystal's band-gap energy. [53].

Minimally-Invasive Real-Time Temperature Monitoring

The beauty of fiber optics is that it provides real-time temperature measurements and is thin and flexible, making insertion into the brain, quite simple. For minimally-invasive FUS thermal ablation with the HIFU probe, a fiber optic temperature sensor could be placed inside a catheter with a needle tip and positioned in the designated area through the already exposed brain tissue. For non-invasive FUS procedures in the brain, a fiber optic temperature sensor could be introduced into the brain via a small burr hole or through the nostril.

Materials and Methods

Selection of Fiber Optic Temperature Sensor

Fiber optics have a wide range of applications throughout several industries including medical, environmental, chemical, microwave and radio-frequency, electrical, etc. A fiber optic temperature sensor that could be used in the CNS would have several requirements:

- Compatible with ethylene oxide sterilization for repetitive pre-clinical testing
- Able to withstand epoxy adhesive coating in order to secure the fiber to a catheter for insertion
- A small bending radius that would not cause significant signal loss, as the fiber may need to be fed through the nostril and into the brain at various angles
- A measurement range of 35-65°C to account for values of human body temperature up to temperatures generated by thermal ablation
- A resolution of at least 0.2°C to monitor the slightest increase in temperature to ensure safety of the patient

- Able to maintain temperature readings within the specified resolution for at least 24 hours

As part of this study, selection of an appropriate fiber optic temperature sensor was determined by extensive product research. Three vendors were selected and their products compared. In Table 4-I, it can be seen that the FISO sensor met all of the requirements, as well as had the smallest diameter - a key component for insertion into the CNS via varying pathways. As a result, the FISO sensor (*Model #:* THR-NS-1165E), shown in Fig. 4-2 was acquired and all experimental analyses discussed here were conducted with the FISO sensor.

Table 4-I. Temperature Sensor Comparison

Parameter	**OpSens** [54]	**Rugged Monitoring** [55]	**FISO** [56]
Outer Diameter (bare fiber)	0.17 mm	0.50 mm	0.155 mm
Outer Diameter (with polyimide tubing)	0.56 mm	—-	0.310 mm
Fiber Length	1.5 m	2 m	2m
Polyimide Tubing Length	0.9 m	—-	1.8 m
Operating Temperature Range	20-85°C	-200 to 250°C	10-90°C
Resolution	0.01°C	0.1°C	0.1°C
Bending Radius	10 mm	400 mm	17 mm
Sterilization Method	Ethylene Oxide	Autoclave	Ethylene Oxide
Epoxy Coating	Yes, on fiber but not on sensor tip	Yes, on fiber but not on sensor tip	Yes, on fiber but not on sensor tip

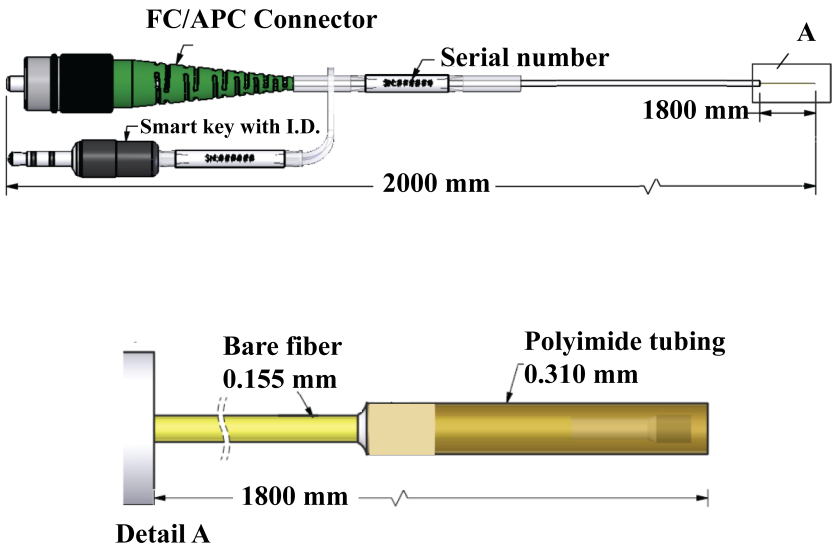

Figure 4-2. FISO Temperature Sensor Schematic (reproduced with permission from [56]).

FISO Materials

The FISO sensor selected was ordered with custom modifications. Rather than typical long insulation covering most of the fiber (which would increase the diameter of the cable), polyimide tubing was placed over the fiber from the connector to almost the sensor tip. The signal conditioner used for this temperature sensor was the SPC-HR reading module designed for research and original equipment manufacturer (OEM) applications and is shown in Fig. 4-3. It consisted of two channels and was cable of sampling at a rate of 125 Hz. Included with the system was the Evolution Software that allowed for configuration and control of reading the sensor, simple monitoring and real-time graphing, as well as exporting of data into multiple formats.

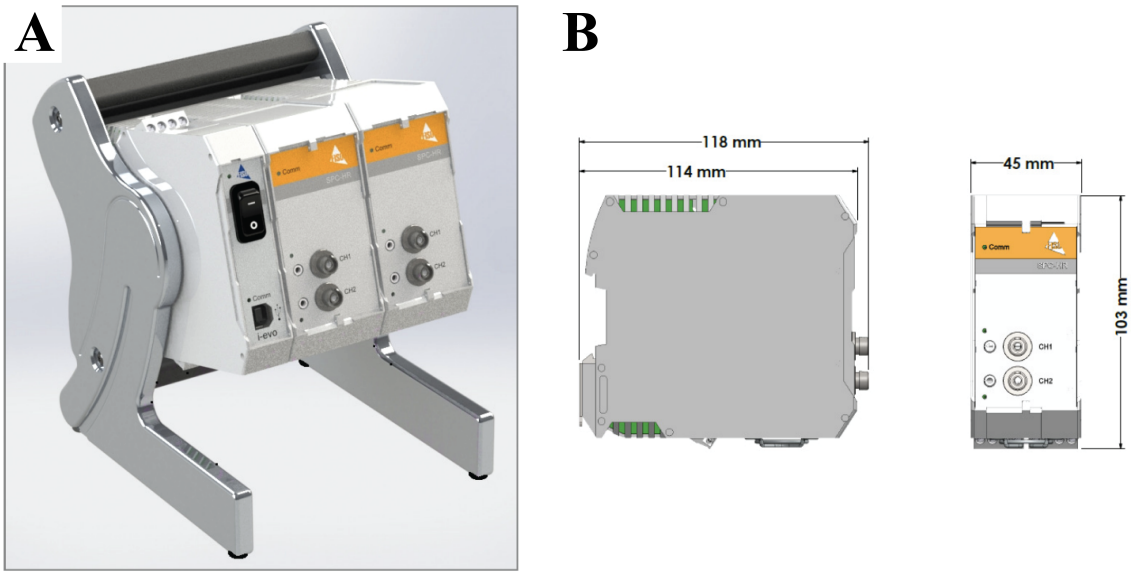

Figure 4-3. (A) FISO Signal Conditioner and (B) Dimensions (reproduced with permission from [56]).

Zero Drift

Zero drift testing verifies the requirement of the temperature sensor to maintain readings within the specified resolution for at least 24 hours. Testing was carried out in a 660 ml water bath held at 37°C for 24 hours. The fiber optic temperature sensor was inserted in a small hole through the water bath lid and secured outside so that the tip could free float but remain clear of the walls and heating element.

Stability of Measurement

The purpose of testing for stability of temperature sensing, is to ensure that other environmental factors do not affect stability of the sensing. Another component of the environment can be varied to visualize unwanted effects. For this test, pressure was chosen. The setup is shown in Fig. 4-3, where a hydrostatic water column was placed inside a temperature-controlled water bath. Temperature was recorded for 30 seconds while the water bath was held at 42°C and the absolute pressure was set to 7.356 mmHg by keeping the water at a height of 10 cm in the column. Temperature

was recorded again for 30 seconds while the water bath remained set at 42°C and the pressure was increased to 13.976 mmHg by raising the water level in the column to 19 cm.

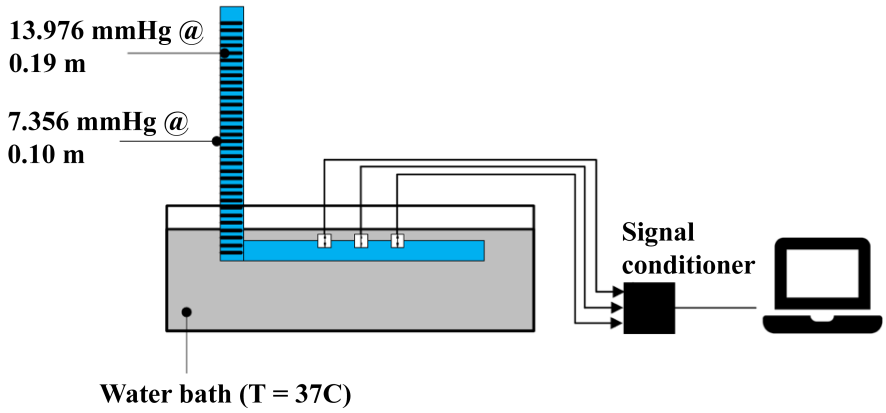

Figure 4-4. Stability of Measurement Test Setup. Water bath kept at 37°C with a hydrostatic water column.

Accuracy

Accuracy testing was carried out in a 660 ml water bath. Temperature was varied between 24-42°C by increments of 2°C. For each temperature point, the fiber optic sensor and two reference sensors measured the water temperature for 5 minutes. The reference sensors' temperature was manually recorded every 30 seconds. This was repeated 3 times for each temperature point. Two Fahrenheit negative temperature coefficient (NTC) temperature sensors, which measure increasing temperature by decreasing resistance, were used as the reference sensors [57].

Bend Radius

To ensure that the sensor remained functional and had no significant loss of signal under various bend radii imposed by the surgeon on the integrated catheter, temperature recording was conducted at bend radii of 8.5 mm, 17 mm, and 30 mm for a test period of 1 hour.

Results and Discussion

Zero Drift Testing

The potential drift of the temperature sensor needed to be evaluated given that many FUS procedures can last on the order of hours. This is particularly important for thermal ablation procedures that need real-time accurate temperature monitoring. Fig. 4-4 shows the results of the 24 hour zero drift test of the fiber optic temperature sensor. The sensor was kept in a temperature-controlled water bath held at 37°C. One can see that there was no significant drift from this temperature over a 24 hour period of time. Further, the mean and standard deviation of the readings were 36.40°C and +/- 0.22, respectively. Temperatures in the thermal ablation range should be tested next.

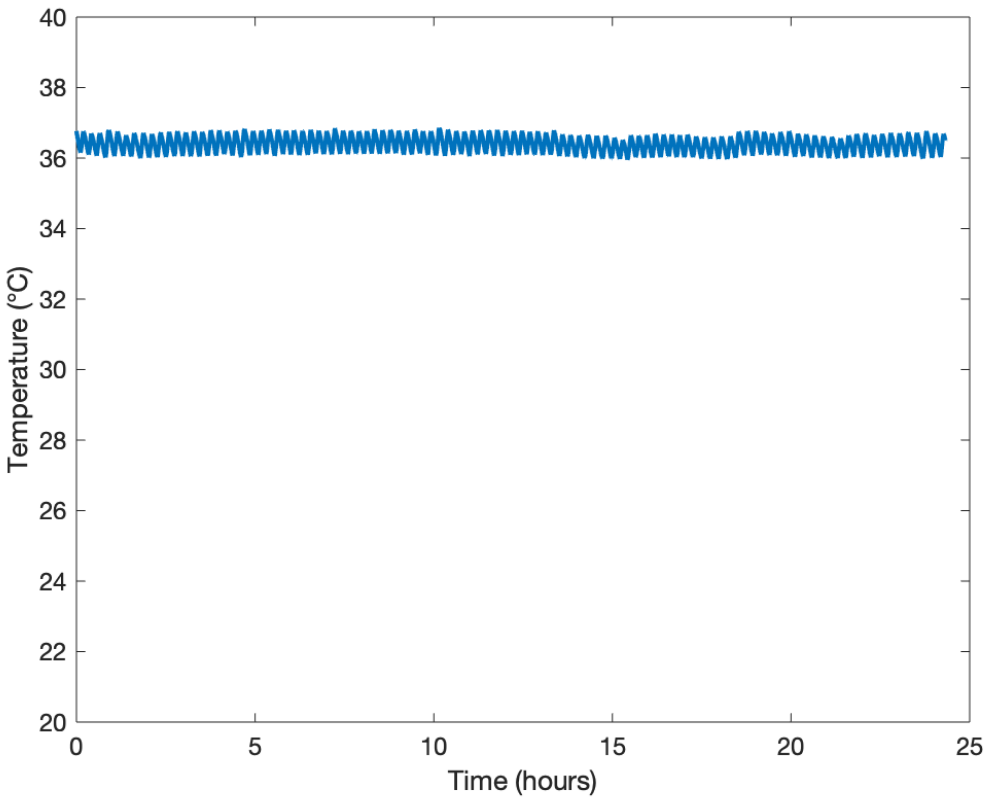

Figure 4-5. Zero Drift Testing Results

Stability of Measurement

During complex procedures, it is important to ensure other environmental variables do not have significant effect on temperature sensing. Pressure variation was used to observe any effects on temperature measurement, although more variables should be varied in future testing. Results of temperature sensor stability are shown in Fig. 4-5. The different pressures did not cause any significant effect on temperature sensing. Even at the greatest gap in readings (between 0 and 10 seconds), the difference was no more than 0.2°C, which equates to the desired resolution requirement for the sensor.

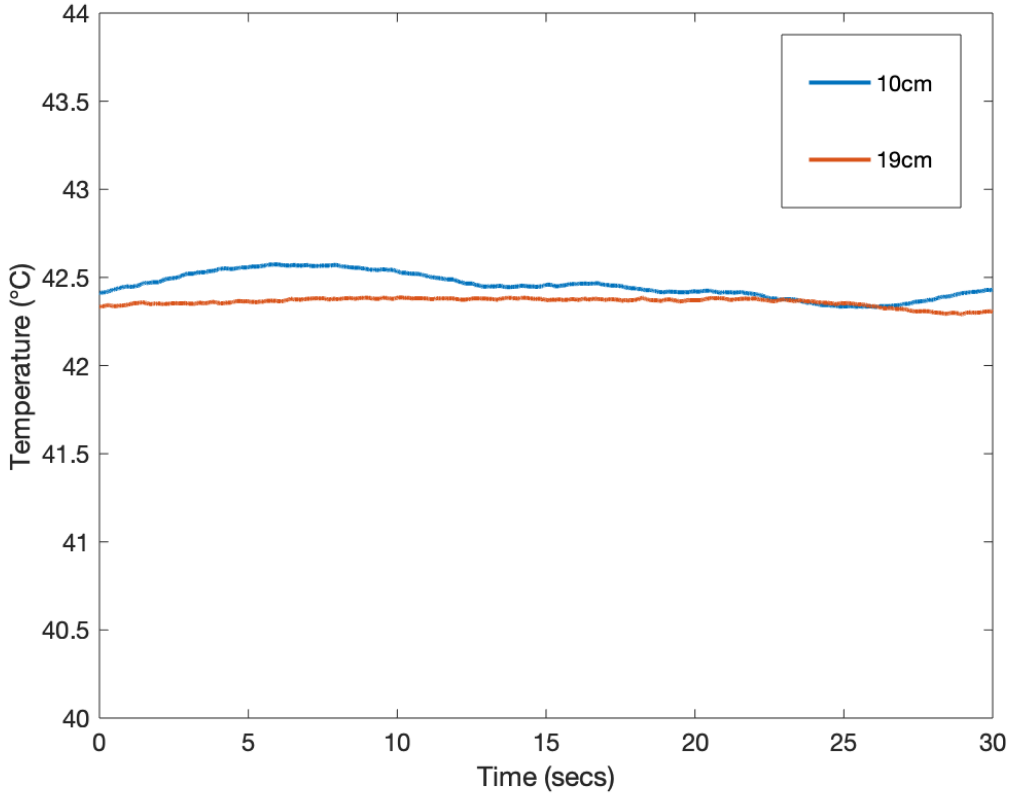

Figure 4-6. Stability of Measurement Testing Results

Accuracy

The FISO temperature sensor chosen was manufactured to have a sensing range of 10-90°C. This covers human body temperature, as well as above and below, which will be sufficient for all types of FUS procedures in the CNS. Since a primary concern of thermal ablation procedures is rising temperature, it is important to ensure the accuracy of the sensor as the medium in which it's in heats. Here, accuracy was tested by varying the water bath temperature between 24-42°C. Two reference sensors were used in conjunction with the fiber optic sensor to gauge its accuracy. Four accuracy temperature plots are shown in Fig. 4-6. At the lower temperatures (26°C and 36°C), the fiber optic sensor remained stable within a 0.2°C variation and recorded quite similar to the reference sensors. At higher temperatures (40°C and 42°C), the fiber optic sensor remained quite stable within a 0.2°C variation, but differed from the reference sensors. This is believed to be due to the reference sensors only having a resolution of 0.1°F between 0-100°F. Higher temperatures above 40 °C are equivalent to 100+°F values, meaning there was only a 1°F resolution during these tests. These tests will be repeated with a platinum resistance sensor as the reference sensor. Higher temperatures in the thermal ablation range will also be tested.

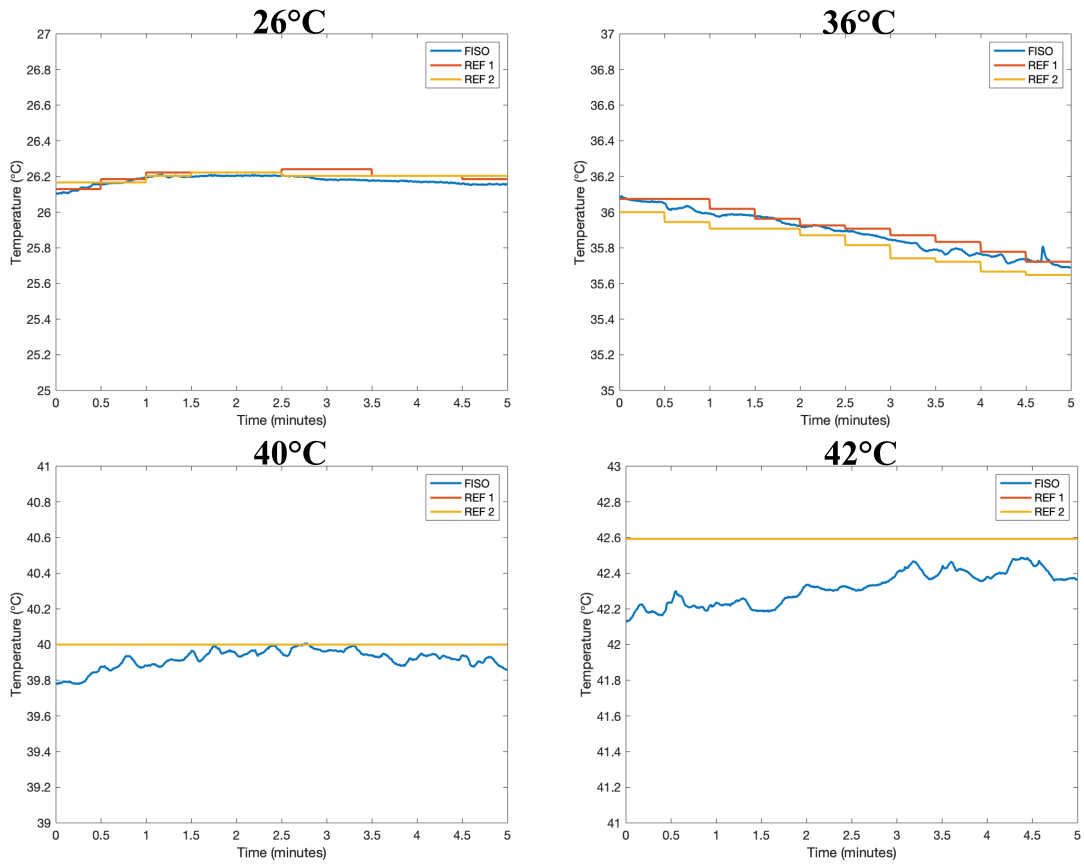

Figure 4-7. Accuracy Testing Results

Bend Radius

Due to the principle of fiber optics in which light travels along the core via TIR, bending the fiber can cause signal loss or incorrect readings. By bending the sensor, light will reflect off the cladding in a different pattern than expected. In order to use a fiber optic sensor within complex FUS procedures, it may need to be routed into the CNS via various pathways that may cause bending. Values at, above, and below the FISO recommended bend radius of 17 mm were tested to determine if bending would cause any significant signal loss and/or incorrect readings. Fig. 4-7 shows the results of the bend radius test in which bend radii of 30 mm, 17 mm, and 8.5 mm were imposed on the fiber while the sensor recorded values for 1 hour in a 37°C water bath. They are in agreement with one another, suggesting that small coils can be

made with this fiber without any signal loss or incorrect readings. Future testing will be conducted in which multiple coils are imposed over a longer recording period.

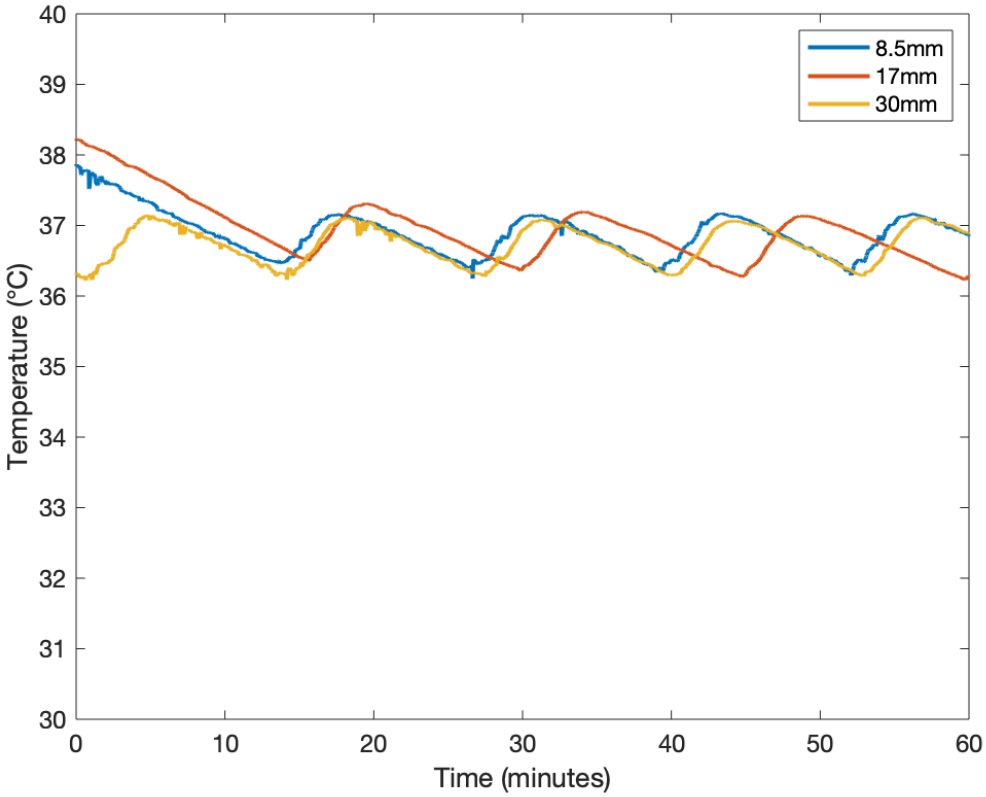

Figure 4-8. Bend Radius Testing Results

Conclusion

The FISO fiber optic temperature sensor presented here has met all requirements necessary for measuring temperature throughout the CNS during FUS procedures based on preliminary testing. Further testing will be conducted to re-evaluate accuracy and bend radius findings, as well as to ensure stability of measurement when exposed to varying environmental factors. Fiber optic sensors are capable of real-time temperature measurements and are thin and flexible, making insertion into the brain, quite simple. For minimally-invasive FUS thermal ablation with the HIFU probe, a fiber optic

temperature sensor could be placed inside a catheter with a needle tip and positioned in the designated area through the already exposed brain tissue. For non-invasive FUS procedures in the brain, a fiber optic temperature sensor could be introduced into the brain via a small burr hole or through the nostril. The next steps will be to test this in small animals.

Conclusions, Limitations, and Future Directions

Conclusions

GBs are the most common malignant primary brain tumors, accounting for 50% of malignant primary brain tumors and 15% of all central nervous system tumors [3]. GBs are aggressive, invasive, and result in the shortest survival rate among malignant brain tumors. There are numerous FUS therapies with the potential to treat GB. More research needs to be conducted for each therapy, and this thesis has explored devices that can be used for most, if not all of them.

The minimally invasive HIFU probe has been designed and fabricated in a way that allows for miniaturization, steering of the focal point, and MR-compatibility. It consisted of a 7mm x 32mm curved transducer, that fit into a 10mm housing. It is capable of fitting into a BrainPath trocar with a diameter of 11mm. Three elements were incorporated into the therapeutic transducer that allows for axial steering when time delays are introduced. The focus can be positioned approximately 4.1-4.5cm away from the transducer. This probe was also designed to be MR-compatible, affording surgeons the ability to use the device with MRI guidance. The miniaturization enables minimally invasive approaches for the treatment of brain lesions, while the steering capabilities of the focal point allow for the treatment of lesions of various sizes. MR-compatibility would pave the path for FUS treatments under MR-guidance. The minimally invasive technique will allow for effective thermal ablation of GB in one

procedure. Although it was designed with thermal ablation in mind, the HIFU probe if coupled properly, has the capability of performing transcranial FUS for less intense therapies (i.e., SDT, BBB opening, radiosensitization, etc.)

Through the phantom study, functionality of the RK-300 was confirmed. The guided focus finding procedure allowed for the focus to be registered at the home position. Treatment planning was successful in that the x,y planes selected for sonication corresponded to the correct axial slice used for real-time MRI. A clear focal point of appropriate size, defined by the manufacturer, was visible with real-time MRI. Providing optimal results in future testing, the RK-300 can be used for several effective GB treatments as well.

The FISO fiber optic temperature sensor presented here has met all of the requirements necessary for measuring temperature throughout the CNS during FUS procedures. It is capable of real-time temperature measurements and is thin and flexible, making insertion into the brain straightforward. For minimally-invasive FUS thermal ablation with the HIFU probe, a fiber optic temperature sensor could be placed inside a catheter with a needle tip and positioned in the designed area through the already exposed brain tissue. For non-invasive FUS procedures in the brain, a fiber optic temperature sensor could be introduced into the brain via a small burr hole or through the nostril. Providing that most types of GB therapies and treatment procedures are lengthy and involve thermal effects, real-time temperature monitoring will serve as a safety mechanism.

Limitations

The HIFU probe presented here will depend on imaging modalities other than ultrasound for guidance. Although designed to be MR-compatible, testing for the probe is still underway to ensure that the strong magnetic fields do not cause heating

of any elements or interference in the performance of the device. Also, the frequency of MRI scans required to guide and monitor the therapy might pose a limitation. The artifact (if any) that the probe would produce in an image would need to be considered. In terms of other imaging modalities, such as CT, additional testing would need to be completed to not only ensure that the probe does not cause excessive artifact, but also whether the probe can withstand X-ray exposure. In addition to imaging limitations, this probe cannot be tested on small animals, since it is designed to fit within the brain of a human. Large animal studies might be possible.

Unfortunately, the generation of a focus within a phantom could not be confirmed with the RK-300. As previously mentioned, the phantom could not be easily coupled to the membrane cuboid with gel, due to the presence of bubbles. The gel was centrifuged to reduce bubbles, but ultimately more bubbles were formed when the gel was expelled and created folds over itself. This led to the phantom being placed inside a water bath, in which it floated slightly. The phantom should have been pressed down firmly and secured to the base of the water bath.

With the goal of using the fiber optic temperature sensor for monitoring of FUS procedures, testing needs to be done to ensure that FUS will not cause any unwanted effects on the fiber. In addition, the water column and bath used for stability of measurement testing is a weaker version of a traditional pressure chamber. A chamber specifically designed for this testing would be best for further work.

Future Directions

The beauty of FUS is that it has endless potential for applications of GB treatment. In turn, this presents the mountain of research that needs to be conducted in order to incorporate this technique into the clinical setting. Preliminary data of a minimally invasive HIFU probe shows promising functionality, but further testing of ablation

capabilities and confirmation of focal steering is still needed. In addition, testing must be conducted in cadavers and large animal models. Visualization of the focus using the RK-300 with MRI indicates the system is fully capable of meeting research needs, but a BBB opening in an animal could serve as confirmation of FUS penetration through the skull before complete animal studies commence. Bench top testing of a fiber optic temperature sensor shows promising results, but animal testing with reference sensors and MR thermometry are needed to confirm its reliable usage in FUS procedures.

At Johns Hopkins, *in vitro* and *in vivo* SDT studies are currently underway and will be the next experiments conducted with the RK-300. *In vitro* studies will confirm the preferential uptake of 5-ALA in human GB cells, access ROS production from SDT, and examine ROS effects on neighboring healthy cells. *In vivo* studies will confirm repeatability of treatment parameters from the Wu et al. study [34], as well as explore the effect of multiple SDT treatments for the same animals, with the goal of complete tumor destruction.

References

[1] "NCI Dictionary of Cancer Terms," Accessed: 2021-04-11. [Online]. Available: https://www.cancer.gov/publications/dictionaries/cancer-terms/def/neoplasm

[2] Q. T. Ostrom, G. Cioffi, H. Gittleman, N. Patil, K. Waite, C. Kruchko, and J. S. Barnholtz-Sloan, "Cbtrus statistical report: Primary brain and other central nervous system tumors diagnosed in the united states in 2012-2016," *Neuro Oncol*, vol. 21, no. Suppl 5, pp. v1–v100, 2019. [Online]. Available: https://www.ncbi.nlm.nih.gov/pubmed/31675094

[3] "Glioblastoma Multiforme," Accessed: 2021-04-11. [Online]. Available: https://www.aans.org/en/Patients/Neurosurgical-Conditions-and-Treatments/Glioblastoma-Multiforme

[4] "Brain Tumor Therapeutics: Global Markets to 2023," Accessed: 2021-04-11. [Online]. Available: https://www.bccresearch.com/market-research/pharmaceuticals/brain-tumor-therapeutics-markets.html

[5] "Radiation Therapy to Treat Cancer," Accessed: 2021-04-11. [Online]. Available: https://www.cancer.gov/about-cancer/treatment/types/radiation-therapy

[6] D. R. Johnson and B. P. O'Neill, "Glioblastoma survival in the united states before and during the temozolomide era," *J Neurooncol*, vol. 107, no. 2, pp. 359–64, 2012. [Online]. Available: https://www.ncbi.nlm.nih.gov/pubmed/22045118

[7] "Chemotherapy," Accessed: 2021-04-11. [Online]. Available: https://www.mayoclinic.org/tests-procedures/chemotherapy/about/pac-20385033

[8] R. Daneman and A. Prat, "The blood-brain barrier," *Cold Spring Harb Perspect Biol*, vol. 7, no. 1, p. a020412, 2015. [Online]. Available: https://www.ncbi.nlm.nih.gov/pubmed/25561720

[9] J. Weingart, "Glioblastoma Multiforme (GBM): Advancing Treatment for a Dangerous Brain Tumor," Accessed: 2021-04-11. [Online]. Available: https://www.hopkinsmedicine.org/health/conditions-and-diseases/glioblastoma-multiforme-gbm-advancing-treatment-for-a-dangerous-brain-tumor

[10] R. M. Young, A. Jamshidi, G. Davis, and J. H. Sherman, "Current trends in the surgical management and treatment of adult glioblastoma," *Ann Transl Med*, vol. 3, no. 9, p. 121, 2015. [Online]. Available: https://www.ncbi.nlm.nih.gov/pubmed/26207249

[11] M. Lara-Velazquez, R. Al-Kharboosh, S. Jeanneret, C. Vazquez-Ramos, D. Mahato, D. Tavanaiepour, G. Rahmathulla, and A. Quinones-Hinojosa, "Advances in brain tumor surgery for glioblastoma in adults," *Brain Sci*, vol. 7, no. 12, 2017. [Online]. Available: https://www.ncbi.nlm.nih.gov/pubmed/29261148

[12] K. L. Chaichana, I. Jusue-Torres, R. Navarro-Ramirez, S. M. Raza, M. Pascual-Gallego, A. Ibrahim, M. Hernandez-Hermann, L. Gomez, X. Ye, J. D. Weingart, A. Olivi, J. Blakeley, G. L. Gallia, M. Lim, H. Brem, and A. Quinones-Hinojosa, "Establishing percent resection and residual volume thresholds affecting survival and recurrence for patients with newly diagnosed intracranial glioblastoma," *Neuro Oncol*, vol. 16, no. 1, pp. 113–22, 2014. [Online]. Available: https://www.ncbi.nlm.nih.gov/pubmed/24285550

[13] D. S. Hersh, A. J. Kim, J. A. Winkles, H. M. Eisenberg, G. F. Woodworth, and V. Frenkel, "Emerging Applications of Therapeutic Ultrasound in Neuro-oncology: Moving Beyond Tumor Ablation," *Neurosurgery*, vol. 79, no. 5, pp. 643–654, 08 2016. [Online]. Available: https://doi.org/10.1227/NEU.0000000000001399

[14] F. A. Jolesz, K. Hynynen, N. McDannold, and C. Tempany, "Mr imaging–controlled focused ultrasound ablation: A noninvasive image-guided surgery," *Magnetic Resonance Imaging Clinics of North America*, vol. 13, no. 3, pp. 545–560, 2005, mR-Guided Interventions. [Online]. Available: https://www.sciencedirect.com/science/article/pii/S1064968905000401

[15] C. Brace, "Thermal tumor ablation in clinical use," *IEEE Pulse*, vol. 2, no. 5, pp. 28–38, 2011.

[16] D. Coluccia, J. Fandino, L. Schwyzer, R. O'Gorman, L. Remonda, J. Anon, E. Martin, and B. Werner, "First non-invasive thermal ablation of a brain tumor with mr guided focused ultrasound," *Journal of therapeutic ultrasound*, vol. 2, p. 17, 10 2014.

[17] O. Murty, "Variability in thickness of skull bones and sternum," *Journal of Forensic Medicine and Toxicology ISSN 0971-1929*, 07 2009.

[18] M. Belzberg, S. Mahapatra, A. Perdomo-Pantoja, F. Chavez, K. Morrison, K. T. Xiong, N. J. Gamo, S. Restaino, N. Thakor, Y. Yazdi, R. Iyer, B. Tyler, N. Theodore, M. G. Luciano, H. Brem, M. Groves, A. R. Cohen, and A. Manbachi, "Minimally invasive therapeutic ultrasound: Ultrasound-guided ultrasound ablation in neuro-oncology," *Ultrasonics*, vol. 108, p. 106210, 2020. [Online]. Available: https://www.ncbi.nlm.nih.gov/pubmed/32619834

[19] M. Belzberg, F. Chavez, K. T. Xiong, K. Morrison, N. Gamo, S. Restaino, R. Iyer, M. Groves, N. Thakor, H. Brem, A. Cohen, and A. Manbachi, "Minimally invasive intraventricular ultrasound: design and instrumentation towards a miniaturized ultrasound-guided focused ultrasound probe," vol. 10951, pp. 770 – 778, 2019. [Online]. Available: https://doi.org/10.1117/12.2513150

[20] "Fda approves new focused ultrasound clinical trial to treat deadly brain tumors," 2019. [Online]. Available: https://www.fusfoundation.org/news/fda-approves-new-clinical-trial-to-treat-deadly-brain-tumors

[21] J. F. Deeken and W. Löscher, "The blood-brain barrier and cancer: Transporters, treatment, and trojan horses," *Clinical Cancer Research*, vol. 13, no. 6, pp. 1663–1674, 2007. [Online]. Available: https://clincancerres.aacrjournals.org/content/13/6/1663

[22] S. Madsen and H. Hirschberg, "Site-specific opening of the blood-brain barrier," *Journal of biophotonics*, vol. 3, pp. 356–67, 06 2010.

[23] "What is definity?" Accessed: 2021-04-19. [Online]. Available: https://www.definityimaging.com/what-is-definity.html

[24] S. Hernot and A. Klibanov, "Microbubbles in ultrasound-triggered drug and gene

delivery," *Advanced drug delivery reviews*, vol. 60, pp. 1153–66, 07 2008.

[25] T. Mainprize, N. Lipsman, Y. Huang, Y. Meng, A. Bethune, S. Ironside, C. Heyn, R. Alkins, M. Trudeau, A. Sahgal, J. Perry, and K. Hynynen, "Blood-brain barrier opening in primary brain tumors with non-invasive mr-guided focused ultrasound: A clinical safety and feasibility study," *Scientific Reports*, vol. 9, 01 2019.

[26] C. Schneider, G. Woodworth, Z. Vujaskovic, and M. Mishra, "Radiosensitization of high-grade gliomas through induced hyperthermia: Review of clinical experience and the potential role of mr-guided focused ultrasound," *Radiotherapy and Oncology*, vol. 142, 08 2019.

[27] J. P. May and S.-D. Li, "Hyperthermia-induced drug targeting," *Expert Opinion on Drug Delivery*, vol. 10, no. 4, pp. 511–527, 2013. [Online]. Available: https://doi.org/10.1517/17425247.2013.758631

[28] A. Novotny and W. Stummer, "5-aminolevulinic acid and the blood-brain barrier – a review," *Medical Laser Application*, vol. 18, no. 1, pp. 36–40, 2003. [Online]. Available: https://www.sciencedirect.com/science/article/pii/S1615161504700848

[29] C. G. Hadjipanayis, G. Widhalm, and W. Stummer, "What is the Surgical Benefit of Utilizing 5-Aminolevulinic Acid for Fluorescence-Guided Surgery of Malignant Gliomas?" *Neurosurgery*, vol. 77, no. 5, pp. 663–673, 08 2015. [Online]. Available: https://doi.org/10.1227/NEU.0000000000000929

[30] S.-G. Zhao, X.-F. Chen, L.-G. Wang, G. Yang, D.-Y. Han, L. Teng, Y. Mingchun, D. Wang, C. Shi, Y.-H. Liu, B.-J. Zheng, C.-B. Shi, X. Gao, and N. Rainov, "Increased expression of abcb6 enhances protoporphyrin ix accumulation and photodynamic effect in human glioma," *Annals of surgical oncology*, vol. 20, 06 2012.

[31] P. Krishnamurthy, G. Du, Y. Fukuda, D. Sun, J. Sampath, K. Mercer, J. Wang, B. Sosa-Pineda, K. Murti, and J. Schuetz, "Identification of a mammalian mitochondrial porphyrin transporter," *Nature*, vol. 443, no. 7111, pp. 586–589, 10 2006.

[32] M.-E. Koller and I. Romslo, "Studies on the uptake of porphyrin by isolated rat liver mitochondria," *Biochimica et Biophysica Acta (BBA) - Bioenergetics*, vol. 503, no. 2, pp. 238–250, 1978. [Online]. Available: https://www.sciencedirect.com/science/article/pii/0005272878901858

[33] N. Rebeiz, S. Arkins, K. W. Kelley, and C. A. Rebeiz, "Enhancement of coproporphyrinogen iii transport into isolated transformed leukocyte mitochondria by atp," *Archives of Biochemistry and Biophysics*, vol. 333, no. 2, pp. 475–481, 1996. [Online]. Available: https://www.sciencedirect.com/science/article/pii/S0003986196904178

[34] S.-K. Wu, M. Santos, S. Marcus, and K. Hynynen, "Mr-guided focused ultrasound facilitates sonodynamic therapy with 5-aminolevulinic acid in a rat glioma model," *Scientific Reports*, vol. 9, 07 2019.

[35] K. Sheehan, D. Sheehan, M. Sulaiman, F. Padilla, D. Moore, J. Sheehan, and Z. Xu, "Investigation of the tumoricidal effects of sonodynamic therapy in malignant glioblastoma brain tumors," *Journal of Neuro-Oncology*, vol. 148, pp. 1–8, 05 2020.

[36] T. T. Wissniowski, J. H‰nsler, D. Neureiter, M. Frieser, S. Schaber, B. Esslinger, R. Voll, D. Strobel, E. G. Hahn, D. Schuppan, and J. H¸nsler, "Activation of tumor-specific t lymphocytes by radio-frequency ablation of the vx2 hepatoma

in rabbits," *Cancer Res*, vol. 63, no. 19, pp. 6496–500, 2003. [Online]. Available: https://www.ncbi.nlm.nih.gov/pubmed/14559842

[37] M. H. den Brok, R. P. Sutmuller, R. van der Voort, E. J. Bennink, C. G. Figdor, T. J. Ruers, and G. J. Adema, "In situ tumor ablation creates an antigen source for the generation of antitumor immunity," *Cancer Res*, vol. 64, no. 11, pp. 4024–9, 2004. [Online]. Available: https://www.ncbi.nlm.nih.gov/pubmed/15173017

[38] Y. Zhang, J. Deng, J. Feng, and F. Wu, "Enhancement of antitumor vaccine in ablated hepatocellular carcinoma by high-intensity focused ultrasound," *World J Gastroenterol*, vol. 16, no. 28, pp. 3584–91, 2010. [Online]. Available: https://www.ncbi.nlm.nih.gov/pubmed/20653069

[39] Z. Hu, X. Y. Yang, Y. Liu, M. A. Morse, H. K. Lyerly, T. M. Clay, and P. Zhong, "Release of endogenous danger signals from hifu-treated tumor cells and their stimulatory effects on apcs," *Biochem Biophys Res Commun*, vol. 335, no. 1, pp. 124–31, 2005. [Online]. Available: https://www.ncbi.nlm.nih.gov/pubmed/16055092

[40] "Glioblastoma multiforme," Accessed: 2021-02-19. [Online]. Available: https://www.aans.org/en/Patients/Neurosurgical-Conditions-and-Treatments/Glioblastoma-Multiforme

[41] "Our integrated system," 2021. [Online]. Available: https://niconeuro.com/our-integrated-system/

[42] M. Acord, T. P. Kaovasia, N. J. Gamo, T. Xiong, E. Curry, F. Aghabaglou, K. Morrison, B. Tyler, M. Luciano, and A. Manbachi, "Design and Fabrication of a Focused Ultrasound Device for Minimally-Invasive Neurosurgery: Reporting a Second, Miniaturized and MR-Compatible Prototype with Steering Capabilities," *American Society of Mechanical Engineers*, vol. 2021 Design of Medical Devices Conference, 2021.

[43] C. S. Kong, "A general maximum power transfer theorem," *IEEE Transactions on Education*, vol. 38, no. 3, pp. 296–298, 1995.

[44] H. Huang and D. Paramo, "Broadband electrical impedance matching for piezoelectric ultrasound transducers," *IEEE Transactions on Ultrasonics, Ferroelectrics, and Frequency Control*, vol. 58, no. 12, pp. 2699–2707, 2011.

[45] "Piezoelectric crystals," 2020. [Online]. Available: https://www.sciencedirect.com/topics/physics-and-astronomy/piezoelectric-crystals

[46] "Piezocad," 2021. [Online]. Available: https://sonicconcepts.com/software/

[47] "Field ii simulation program," 2021. [Online]. Available: https://field-ii.dk/

[48] J. A. Jensen and N. B. Svendsen, "Calculation of pressure fields from arbitrarily shaped, apodized, and excited ultrasound transducers," *IEEE Transactions on Ultrasonics, Ferroelectrics, and Frequency Control*, vol. 39, no. 2, pp. 262–267, 1992.

[49] M. Y. Wang, J. L. Cheng, Y. H. Han, Y. L. Li, J. P. Dai, and D. P. Shi, "Measurement of tumor size in adult glioblastoma: classical cross-sectional criteria on 2d mri or volumetric criteria on high resolution 3d mri?" *Eur J Radiol*, vol. 81, no. 9, pp. 2370–4, 2012. [Online]. Available: https://www.ncbi.nlm.nih.gov/pubmed/21652157

[50] "Mri-guided fus (small bore systems)," 2020. [Online]. Available: https://www.fusinstruments.com/fus-for-high-field-mri-systems-rk-3

[51] "Fda approves first mri-guided focused ultrasound device to treat essential tremor,"

2016. [Online]. Available: https://www.fda.gov/news-events/press-announcements/fda-approves-first-mri-guided-focused-ultrasound-device-treat-essential-tremor

[52] "Fiber-optical thermometer," accessed: 2021-04-13. [Online]. Available: https://www.wikiwand.com/en/Fiber-optical_thermometer

[53] U. Roland, C. Renschen, D. Lippik, F. Stallmach, and F. Holzer, "A new fiber optical thermometer and its application for process control in strong electric, magnetic, and electromagnetic fields," *Sensor Letters*, vol. 1, pp. 93–98, 12 2003.

[54] "Fiber optic temperature sensors," 2020. [Online]. Available: https://opsensmedical.com/products/oem-lifescience-solutions/fiber-optic-temperature-sensors/

[55] "Lsensb fiber optic temperature sensors," accessed: 2021-04-13. [Online]. Available: https://www.ruggedmonitoring.com/product-details/lsensb/5c332aaa517e29000166919a

[56] "Medical: Miniature fiber optic pressure transducers," accessed: 2021-04-13. [Online]. Available: https://fiso.com/en/service/medical/

[57] "Dc 4-28v red+blue fahrenheit dual display digital thermometer with 2 ntc waterproof metal probes temperature sensor," accessed: 2021-04-13. [Online]. Available: http://www.icstation.com/redblue-fahrenheit-dual-display-digital-thermometer-with-waterproof-metal-probes-temperature-sensor
html

Appendix I

MRI Sequence Parameters

Table I-I. MRI Parameters

Parameter	Focus Registration	Phantom Registration	Sonication
Scan Type	T1-weighted FLASH	T1-weighted FLASH	T1-weighted FLASH
Slice Thickness	1 mm	1 mm	1 mm
Number of Slices	5-6	10-12	1
Gap Between Slices	0 mm	0 mm	N/A
FOV	60x60 mm	60x60 mm	70x70 mm
Echo Time (TE)	2.1 ms	2.1 ms	20 ms
Repetition Time (TR)	120 ms	128 ms	39 ms
Acquisition Matrix	200x200 pixels	200x200 pixels	128x128 pixels
Flip Angle	N/A	N/A	20

MOLLY ACORD

525 North Charles Street, Apt 202, Baltimore, MD 21201 | +1 (304) 573 - 8914 | macord1@jh.edu

SUMMARY: Passionate and driven M.S.E. Biomedical Engineering Candidate at Johns Hopkins University with a B.S. in Chemical Engineering. Dedicated researcher preparing for a thesis exploring focused ultrasound applications in neuro-oncology. Accomplished and well-rounded leader with experience ranging from lab research to industry. Enthusiastic and committed team member.

EDUCATION

Johns Hopkins University, Whiting School of Engineering — Baltimore, MD
Master of Science and Engineering in Biomedical Engineering — (Expected May 2021)
GPA: 3.40/4.00

Virginia Tech — Blacksburg, VA
Bachelor of Science in Chemical Engineering — (Aug 2014 – Dec 2018)
Minors in Biomedical Engineering and Chemistry
GPA: 3.15/4.00

Technical University of Denmark — Lyngby, Denmark
Unit Operations Laboratory — (July 2017 – Aug 2017)

- Completed six experiments and plant scale-up design project
- Participated in excursions to world leading chemical production sites to see theories put into action

RELEVANT COURSEWORK

Principles of Design of Biomedical Instrumentation, Medical Imaging Systems, Design of Biomedical Instruments and Systems, Neural Implants and Interfaces, Software Carpentry, MR Imaging in Medicine, Radiology for Engineers

EXPERIENCE

Graduate Researcher — (Sept 2019 – Present)
Neuro-Acoustics Laboratory (Manbachi Lab), Johns Hopkins Medicine — Baltimore, MD
Literature Review:

- Writing a comprehensive literature review regarding current treatment options and potential focused ultrasound treatment options of glioblatoma multiforme (GBM)

Thesis Project:

- Designing a sonodynamic therapy experiment for the treatment of glioblastomas (in-vitro and in-vivo studies)
- Developing a stanard operating procedure (SOP) for an MR guided fcoused ultrasound system (RK-300)

Defense Advanced Research Projetcs Agency (DARPA) Grant for Spinal Cord Injury Management and Treatment:

- Researching, selecting, and testing fiber optic temperature sensor for Acute CSF Management Implant (smart drainage catheter)

Biology Researcher — (Jan 2019 – July 2019)
International Scientific Technologies — Radford, VA
Department of Defense (DOD) Grant for Security Device Development:

- Created reduced graphene oxide films coated with polyoxometalates
- Investigated sensitivity and selectivity of films to four common common gasses found in human breath
- Performed vapor tests at various concentrations of said gasses to detect changes in resistence of the films

Undergraduate Researcher — (Aug 2018 – Dec 2018)
Therapeutic Ultrasound and Noninvasive Therapies Laboratory (Vlaisavljevich Lab), Virginia Tech — Blacksburg, VA

- Optimized focused ultrasound parameters for DNA extraction of salmon tissue and timber
- Performed traditional DNA extraction for comparison
- Analyzed data for future development of portable focused ultrasound DNA extraction device

Chemical Engineering Intern (Glycolic Acid Production) — **(**May 2018 – Aug 2018)
The Chemours Company — Bell, WV

- Led project to install ventilation and fume capture in acid drum plant
- Created standard operating conditions (SOC) for heat trace alarms
- Calculated throughput capacity for all process equipment
- Inspected files, ensuring they had all required information as part of the Mechanical Quality Assurance Initiative

Undergraduate Researcher — (Oct 2017 – May 2018)
Institute for Critical Technology and Applied Science (ICTAS), Virginia Tech — Blacksburg, VA
Research Experience for Undergraduates (REU) Grant to study the structure, function, and mimicry of biological surfaces

- Performed cell culturing and plating on capillary-like surfaces
- Investigated properties of these surfaces using a quartz crystal microbalance with fibronectin coating
- First author poster presenter at the Student Experiential Learning Conference

Undergraduate Researcher — (Sept 2016 – Dec 2017)
Lee Laboratory, Virginia Tech — Blacksburg, VA
Drug Delivery, Autism Spectrum Disorder (ASD), and Lupus Studies

- Quantified behavioural and social data of ASD test subjects
- Prepared dihydrothidium (DHE) stains of ASD brain samples and observed reactive oxidative stress present
- Assisted with tissue collection from ASD and Lupus test subjects
- Co-author poster presentor for School of Biomedical Engineering and Sciences Symposium

PROJECTS

Materal Health Monitor — (Sept 2019 – Dec 2019)

- Researched main causes of materal mortality
- Designed a wearable health monitor to measure heart rate, temperature, and blood pressure

- Wrote Arduino algorithm to measure heart rate and temperature
- Assembled and integrated all electrical components into a prototype

Communication for Quadriplegics (Nov 2019)
- Wrote an Arduino algorithm to implement text based on inputs from joystick sensors
- Assembled and integrated all electrical components into the system

REM Sleep Eye Mask Tracker (Oct 2019)
- Identified piezo resistors as the sensors to be used for detection of eye movement through eyelids
- Assembled and integrated all electrical components into the system

Removal of Carbon Dioxide from the Atmosphere (Jan 2018 – May 2018)

Senior Design Project with MATRIC in Charleston, WV
- Calculated 1% of how much CO_2 must be captured to maintain a constant atmospheric pressure worldwide
- Researched and developed a solid adsorption with temperature swing process to remove CO_2
- Designed and simulated a chemical plant for this process

PUBLICATIONS

- Molly Acord, Tarana Kaovasia, Nao Gamo, Tim Xiong, Kyle Morrison, Betty Tyler, Mark Luciano and Amir Manbachi, **'Design and Fabrication of a Focused Ultrasound Device for Minimally-Invasive Neurosurgery: Reporting a Second, Miniaturized and MR-Compatible Prototype with Steering Capabilities'**, Design of Medical Devices Conference, 2021.
- Smruti Mahapatra, Tarana Parvez Kaovasia, Sufia Maryam Ainechi, Ana Ainechi, Molly Acord, Betty Tyler, Nicholas Theodore and Amir Manbachi, **'Design of an Ultrasound Probe Holder to Minimize Motion Artifact During Sonography'**, Design of Medical Devices Conference, 2021.
- Ana Ainechi, Beth Smith, Jennifer Son, Javad Azadi, Smruti Mahapatra, Molly Acord, Tarana Kaovasia, Betty Tyler, Nicholas Theodore and Amir Manbachi, **'How can ultrasound detect microcirculation? A study of frequency requirements to enable visualization of microvasculature and tissue perfusion.'**, Design of Medical Devices Conference, 2021.
- Manish Balamurugan, Kathryn Chung, Smruti Mahapatra, Molly Acord, Tarana Parvez Kaovasia, Aliaksei Pustavoitau, and Amir Manbachi **'USDL-OD: A Novel YOLOv4 Model Implementation for Minimizing Cotton Retention during Neurosurgical Procedures using Ultrasound Imaging**, The International Scoiety for Optics and Photonics (SPIE), 2020.

COMPUTER SKILLS

- Windows 10
- macOS Catalina
- Microsoft Office
- MATLAB
- Python 3.7
- 3D Slicer
- ImageJ
- Minitab
- Aspen Plus
- SOLIDWORKS

LEADERSHIP SKILLS

Peer Leader (Dec 2017 – Dec 2018)

Center for the Enhancement of Engineering Diversity, Virginia Tech Blacksburg, VA
- Organized professional development events for freshmen and mentors
- Interviewed and hired peer mentors every
- Evaluated weekly reports from mentors each week during the fall semesters

Peer Mentor (Aug 2015 – Nov 2017)

Center for the Enhancement of Engineering Diversity, Virginia Tech Blacksburg, VA
- Mentored 8-10 freshmen engineering students each fall
- Women Engineering Support Team (WEST) mentor
- Coordinated weekly meetings with mentees and provided Peer Leader with weekly reports

ACTIVITIES

Alpha Chi Sigma (AXΣ) – Professional Chemistry Fraternity (April 2016 – May 2018)

Virginia Tech Blacksburg, VA
- Offered free tutoring for general chemistry and organic chemistry
- Performed weekly science experiments at local elementary school
- Visited local nursing home regularly
- Volunteered as a dog walker at animal shelter

Virginia Tech BIG EVENT (April 2015, April 2016, April 2017)

Blacksburg, VA
- Annual day og giving back to the Blacksburg Community
- Volunteer projects ranging from yard work to house painting
- Group leader for three consecutive years

Virginia Tech Relay for Life (April 2016, April 2017, April 2018)

Blacksburg, VA
- First ranked and largest collegiate Relay for Life
- Represented AXΣ and raise money through face painting and bake sales

HONORS

Leslie C. Gates Family Scholarship (2014 – 2015)

Virginia Tech Dean's List Fall 2014, Spring 2018, and Fall 2018

Biographical sketch

Molly Acord is graduating with a Master of Science in Engineering degree in the field of Biomedical Engineering from The Johns Hopkins University. Here she has developed her skills as a researcher in the area of focused ultrasound. Her primary interest is the treatment of glioblastoma.

Molly holds a Bachelor of Science in the field of Chemical Engineering from Virginia Polytechnic Institute and State University. There she performed research in many areas including autism spectrum disorder treatment, mimicry of biological surfaces, and focused ultrasound.

Upon graduation, Molly will transition to industry at a focused ultrasound company in the Baltimore area.

Outside of research, she spends most of her time with her cat, tending to her plants, and cooking.